



저작자표시-비영리-변경금지 2.0 대한민국

이용자는 아래의 조건을 따르는 경우에 한하여 자유롭게

- 이 저작물을 복제, 배포, 전송, 전시, 공연 및 방송할 수 있습니다.

다음과 같은 조건을 따라야 합니다:



저작자표시. 귀하는 원저작자를 표시하여야 합니다.



비영리. 귀하는 이 저작물을 영리 목적으로 이용할 수 없습니다.



변경금지. 귀하는 이 저작물을 개작, 변형 또는 가공할 수 없습니다.

- 귀하는, 이 저작물의 재이용이나 배포의 경우, 이 저작물에 적용된 이용허락조건을 명확하게 나타내어야 합니다.
- 저작권자로부터 별도의 허가를 받으면 이러한 조건들은 적용되지 않습니다.

저작권법에 따른 이용자의 권리는 위의 내용에 의하여 영향을 받지 않습니다.

이것은 [이용허락규약\(Legal Code\)](#)을 이해하기 쉽게 요약한 것입니다.

[Disclaimer](#)

Thesis for the Degree of Master of Science

Anti-diabetic and anti-Alzheimer's disease
potentials of aerial parts of *Epimedium*
koreanum Nakai and its constituents



by

Da Hye Kim

Department of Food and life Science

The Graduate School

Pukyong National University

February 2017

Anti-diabetic and anti-Alzheimer's disease potential
of aerial parts of *Epimedium koreanum* Nakai and its
constituents

(음양곽의 항당뇨 및 항알츠하이머 질환의
활성성분 연구)

Advisor: Prof. Jae Sue Choi

by

Da Hye Kim

A thesis submitted in partial fulfillment of the requirements
for the degree of

Mater of Science

in Department of Food and Life Science, The Graduate School,
Pukyong National University

February 2017

Anti-diabetic and anti-Alzheimer's disease potential of aerial parts of
Epimedium koreanum Nakai and its constituents

A dissertation

by

Da Hye Kim

Approved by:



(Chairman) Taek Jeong Nam



(Member) Un Ju Jung



(Member) Jae Sue Choi

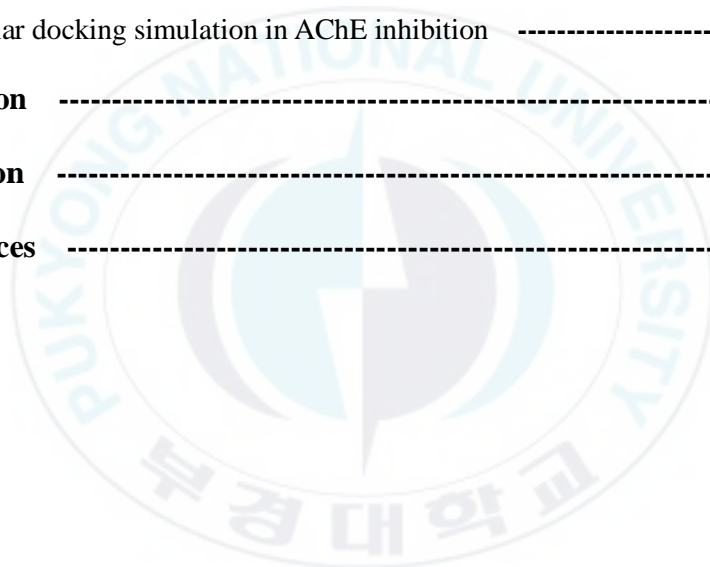
February 24, 2017

Contents

List of Schemes	iv
List of Figures	v
List of Tables	ix
Abbreviations	xi
Abstract	xiii
I. Introduction	1
II. Materials and methods	6
1. Plant materials	6
2. General experimental procedures	7
3. Chemicals and reagents	7
4. Experiment methods	8
4-1. Extraction and fractionation	8
4-2. Isolation of compounds	10
4-2-1. Isolation of compounds from the CH ₂ Cl ₂ fraction	10
4-2-2. Isolation of quercetin from the EtOAc fraction	12
4-2-3. Isolation of icariin from the <i>n</i> -BuOH fraction	14

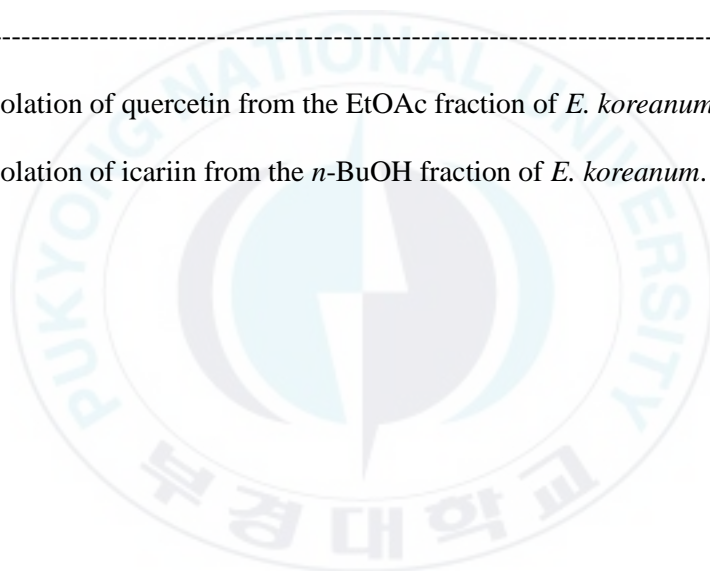
4-3. Anti-diabetic experiments	17
4-3-1. PTP1B inhibitory assay	17
4-3-2. α -Glucosidase Inhibitory assay	19
4-3-3. Enzyme kinetic analysis with PTP1B	21
4-4. Anti-Alzheimer's disease experiments	22
4-4-1. BACE1 inhibitory assay	22
4-4-2. AChE and BChE inhibitory assay	24
4-4-3. Enzyme kinetic analysis with AChE	26
4-5. Molecular docking simulation	27
4-5-1. Molecular docking simulation in PTP1B inhibition	27
4-5-2. Molecular docking simulation in BACE1 inhibition	27
4-5-3. Molecular docking simulation in AChE inhibition	28
5. Statistical analysis	29
III. Results	30
1. Anti-diabetic activity	30
1-1. PTP1B and α -glucosidase inhibitory activities of the MeOH extract and its solvent soluble fractions from aerial parts of <i>E. koreanum</i>	30
1-2. PTP1B and α -glucosidase inhibitory activities of the compounds	34
1-3. Enzyme kinetic analysis of compounds with PTP1B	36
1-4. Molecular docking simulation in PTP1B inhibition	39

2. Anti-Alzheimer's disease activity -----	44
2-1. BACE1 and ChEs inhibitory activities of the MeOH extract and its fractions from aerial parts of <i>E. koreanum</i> -----	44
2-2. BACE1 and ChEs inhibitory activities of the compounds -----	48
2-3. Molecular docking simulation in BACE1 inhibition -----	50
2-4. Enzyme kinetic analysis of compounds with AChE -----	55
2-5. Molecular docking simulation in AChE inhibition -----	59
IV. Discussion -----	64
V. Conclusion -----	74
VI. References -----	75



List of Schemes

Scheme	Page
Scheme 1. Extraction and fractionation of aerial parts of <i>E. koreanum</i> . -----	9
Scheme 2. Isolation of compounds from the CH ₂ Cl ₂ fraction of <i>E. koreanum</i> . - -----	11
Scheme 3. Isolation of quercetin from the EtOAc fraction of <i>E. koreanum</i> . ----	13
Scheme 4. Isolation of icariin from the <i>n</i> -BuOH fraction of <i>E. koreanum</i> . -----	15



List of Figures

Figure	Page
Figure 1. <i>Epimedium koreanum</i> Nakai (Korean Yin Yang Huo). -----	6
Figure 2. Chemical structures of compounds. -----	16
Figure 3. Enzymatic principle of the PTP1B inhibitory assay. -----	18
Figure 4. Enzymatic principle of the α -glucosidase inhibitory assay. -----	20
Figure 5. Enzymatic principle of BACE1 inhibitory assay. -----	23
Figure 6. Enzymatic principle of ChEs inhibitory assay. -----	25
Figure 7. Inhibitory activities of the MeOH extract from <i>Epimedium koreanum</i> on (A) PTP1B, (B) α -glucosidase. All values are expressed as mean \pm S.E.M of triplicate experiments. Ursolic acid and acarbose were used as positive control. -----	33
Figure 8. Dixon and Lineweaver-Burk plots of the inhibition of PTP1B by icaritin and icariside II. The results showed the effects of the presence of different concentrations of the substrate (2.0 mM (●), 1.0 mM (○) and 0.5 mM (▼) for (A) icaritin and 4.0 mM (●), 2.0 mM (○) and 1.0 mM (▼) for (C) icariside II) and the effect of the presence of different concentration of (B) icaritin (0 μ M (●), 2.72 μ M (○), 13.59 μ M (▼)	

and 67.93 μM (Δ)) and (D) icariside II (0 μM (\bullet), 1.94 μM (\circ), 9.73 μM (\blacktriangledown) and 48.64 μM (Δ)). ----- 38

Figure 9. Molecular docking of PTP1B inhibition by compounds (compound 23, compound 2, icaritin and icariside II). Binding site residues of test compounds (compound 23, compound 2, icaritin and icariside II) are represented by *blue*, *black*, *red* and *green* colored structures, respectively. ----- 42

Figure 10. Molecular docking models for PTP1B inhibition of compound 2 (A), icaritin (B) and icariside II (C). ----- 43

Figure 11. Inhibitory activities of the MeOH extract from *Epimedium koreanum* on AChE (A), BChE (B). All values are expressed as mean \pm S.E.M of triplicate experiments. Berberine was used as positive control. ----- 47

Figure 12. Molecular docking of BACE1 inhibition by compounds (QUD, TMF, icaritin and icariside II). Binding sites of test compounds (QUD, TMF, icaritin and icariside II) are represented by *blue*, *black*, *red* and *green* colored structures, respectively. ----- 53

Figure 13. Molecular docking models for BACE1 inhibition of QUD (A), TMF (B), icaritin (C) and catalytic inhibition mode (D) and allosteric inhibition mode (E) of icariside II. These 2D diagrams displayed the binding residues of catalytic inhibition (A, C, D) and allosteric

inhibition (B, E). ----- 54

Figure 14. Dixon and Lineweaver-Burk plots of the inhibition of AChE by icariin and icaritin. The results showed the effects of the presence of different concentrations of the substrate (0.6 mM (●), 0.3 mM (○) and 0.1 mM (▼) for (A) icariin and (C) icaritin and the effect of the presence of different concentration of (B) icariin (0 μM (●), 1.15 μM (○), 5.76 μM (▼) and 28.82 μM (Δ)) and (D) icaritin (0 μM (●), 2.17 μM (○), 10.87 μM (▼) and 54.35 μM (Δ)). ----- 57

Figure 15. Dixon and Lineweaver-Burk plots of the inhibition of AChE by epimedlin A, epimedlin B and epimedlin C. The results showed the effects of the presence of different concentrations of the substrate (0.6 mM (●), 0.3 mM (○) and 0.1 mM (▼) for (A) epimedlin A, (C) epimedlin B and (E) epimedlin C and the effect of the presence of different concentration of (B) epimedlin A (0 μM (●), 4.87 μM (○), 24.33 μM (▼) and 121.65 μM (Δ)), (D) epimedlin B (0 μM (●), 4.95 μM (○), 24.75 μM (▼) and 123.76 μM (Δ)) and (F) epimedlin C (0 μM (●), 4.87 μM (○), 24.33 μM (▼) and 121.65 μM (Δ)). ----- 58

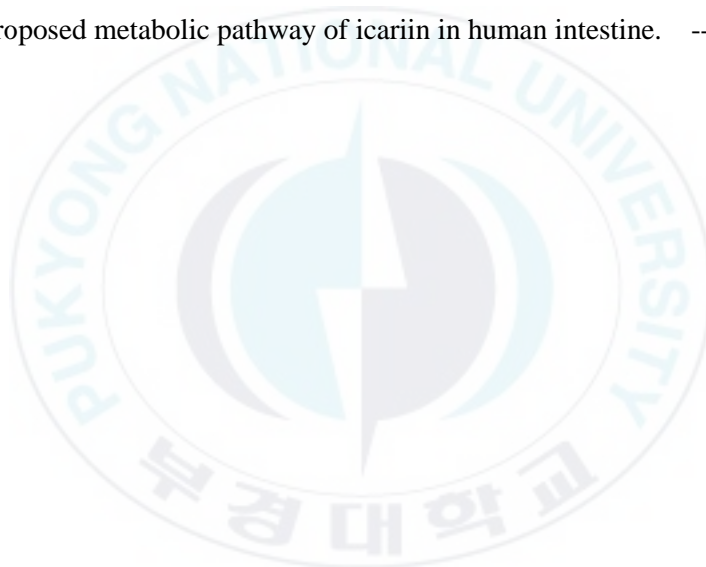
Figure 16. Molecular docking of AChE inhibition by compounds (Tacrine, E2020, icariin, icaritin, epimedlin A, epimedlin B and epimedlin C). Binding site residues of test compounds (Tacrine, E2020, icariin, icaritin,

epimedin A, epimedin B and epimedin C) are represented by *red*,
black, *white*, *purple*, *green*, *blue* and *yellow* colored structures,
respectively. ----- 62

Figure 17. Molecular docking models for AChE inhibition of E2020 (A), icariin
(B), icaritin (C), epimedin A (D), epimedin B (E) and epimedin C (F).

----- 63

Figure 18. Proposed metabolic pathway of icariin in human intestine. ----- 73



List of Tables

Table	Page
Table 1. Inhibitory activities of the MeOH extract and its fractions from <i>Epimedium koreanum</i> on PTP1B and α -glucosidase -----	32
Table 2. Inhibitory activities of compounds of <i>Epimedium koreanum</i> on PTP1B and α -glucosidase -----	35
Table 3. Enzyme kinetic analysis of compounds of <i>E. koreanum</i> with PTP1B --- -----	37
Table 4. Binding site residues and docking scores of compounds in protein tyrosine phosphatase 1B (PTP1B) using AutoDock 4.2 program -----	41
Table 5. Inhibitory activities of the MeOH extract and its fractions from <i>Epimedium koreanum</i> on BACE1 and ChEs -----	46
Table 6. Inhibitory activities of compounds of <i>Epimedium koreanum</i> on BACE1 and ChEs -----	49
Table 7. Binding site residues and docking scores of compounds in β -site APP cleaving enzyme 1 (BACE1) using AutoDock 4.2 program -----	52
Table 8. Enzyme kinetic analysis of compounds of <i>E. koreanum</i> with AChE ---- -----	56

Table 9. Binding site residues and docking scores of compounds in acetylcholinesterase (AChE) using AutoDock 4.2 program ----- 61



Abbreviations

A β	: Amyloid β
ACh	: Acetylcholine
AChE	: Acetylcholinesterase
AD	: Alzheimer's disease
ADT	: AutoDock Tool
AGI	: α -Glucosidase inhibitor
APP	: Amyloid precursor protein
ATCh	: Acetylthiocholine iodide
BACE1	: β -site amyloid precursor protein cleaving enzyme 1
BChE	: Butyrylcholinesterase
BTCh	: Butyrylthiocholine chloride
BuOH	: Butanol
CC	: Column chromatography
CDCl ₃	: Deuterium chloroform
CH ₂ Cl ₂	: Dichloromethane
ChE	: Cholinesterase
ChEI	: Cholinesterase inhibitor
Compound 2	: 3-(3,5-dibromo-4-hydroxy-benzoyl)-2-ethyl- benzofuran-6-sulfonic acid (4-sulfamoyl-phenyl)-amide
Compound 23	: 3-({5-[(N-acetyl-3-{4-[(carboxycarbonyl)(2-carboxyphenyl)amino]-1-naphthyl}-L-alanyl)amino]pentyl}oxy)-2-naphthoic acid
DM	: Diabetes mellitus

DMSO	: Dimethyl sulfoxide
DTNB	: 5,5'-Dithio-bis-(2-nitrobenzoic acid)
DTT	: Dithiothreitol
<i>E. koreanum</i>	: <i>Epimedium koreanum</i> Nakai
EDTA	: Ethylenediaminetetraacetic acid
EH	: Epimedii Herba
EI-MS	: Electron impact ionization mass spectrometry
EtOAc	: Ethyl acetate
GA	: Genetic algorithm
IC ₅₀	: Half inhibitory concentration
IR	: Insulin receptor
IRS	: Insulin receptor substrate
SAR	: Structure activity relationship
SI	: Selectivity index
Si gel	: Silica gel
K _i	: Inhibition constant
<i>p</i> NPG	: <i>p</i> -Nitrophenyl α -D-glucopyranoside
<i>p</i> NPP	: <i>p</i> -Nitrophenyl phosphate
PAS	: Peripheral anionic site
PTP1B	: Protein tyrosine phosphatase 1B
QUD	: 2 - amino - 3 - { (1R) - 1 - cyclohexyl - 2 - [(cyclohexylcarbonyl) amino] ethyl } - 6 -phenoxyquinazolin-3-ium
TCM	: Traditional Chinese medicine
TLC	: Thin layer chromatography
TMF	: 5,7,4'-trimethoxyflavone
UV	: Ultraviolet

음양곽의 항당뇨 및 항알츠하이머 질환의 활성성분 연구

김 다 혜

부경대학교 대학원 식품생명과학과

요 약

당뇨병은 전 세계적으로 발생하고, 그 발생빈도는 대부분의 국가에서 빠르게 증가 하고 있다. Protein tyrosine phosphatase 1B (PTP1B)는 활성화된 인슐린 수용체의 티로신 잔기를 탈인산화 시킴으로써 인슐린 저항성을 조절하고, α -glucosidase는 소장에서 탄수화물의 흡수를 지연시켜 혈당량과 인슐린 감소에 관여 하는 효소이다. 따라서, 천연물로부터 분리한 PTP1B와 α -glucosidase의 저해제는 당뇨병의 예방과 치료에 중요할 것으로 생각된다. 뿐만 아니라, 전 세계의 4,600 만 명이 신경퇴행성 질환인 알츠하이머 질환을 앓고 있으며, 이 또한 앞으로 빠르게 증가할 것이다. β -site amyloid precursor protein cleaving enzyme 1 (BACE1)은 아밀로이드 전구체 단백질 (APP)의 β -site를 절단하여 아밀로이드 베타 ($A\beta$)를 생성을 조절하고, acetylcholinesterase (AChE)와 butyrylcholinesterase (BChE)는 알츠하이머 발병에 관여하는 중요한 신경전달 물질인 acetylcholine (ACh)을 조절하는 효소이므로, 이 효소들의 저해제는 알츠하이머 질환의 예방 및 치료에 중요한 역할을 할 것이다. 음양곽 (淫羊藿)은 매자나무과에 속하는 다년생 초본식물인 삼지구엽초의 전초를 말린 것으로, 한방에서는 성호르몬 장애, 이뇨 작용 및 혈압 강하 작용 등에 쓰인다. 그러나 항당뇨 및 항 알츠하이머 효과에 대해서는 잘 알려져 있지 않으므로 이번 연구에서는 음양곽과 그 구성성분의 항 당뇨 및 항알츠하이머 효과를 확인하였다. 음양곽의 MeOH 추출물, 극성에 따른 분획물 및 화합물들의 PTP1B, α -glucosidase, BACE1, AChE 및 BChE에 대한 저해 활성을 평가하고, 활성을 나타내는 화합물의 효소반응속도 연구와 분자 도킹 시뮬레이션을 통하여 저해제로서의 가능성을 확인하였다. 모든 실험에서

CH₂Cl₂ 분획물이 가장 높은 저해 활성을 보였으며, BACE1 억제 활성 평가를 제외한 실험에서 EtOAc 및 *n*-BuOH 분획물이 CH₂Cl₂ 분획물 다음으로 좋은 활성을 나타냈다. 활성을 측정한 화합물 중 icaritin 및 icariside II가 각각 11.59 ± 1.39 및 9.94 ± 0.15의 IC₅₀ 값을 보이며 PTP1B에 대한 억제 활성을 나타냈고, 74.42 ± 0.01 및 106.59 ± 0.44의 IC₅₀ 값을 보이며 α-glucosidase 억제에 좋은 효과를 보였다. 반면에, icariin, epimedin A, epimedin B, epimedin C, magnolol 및 (-)-syringaresinol은 억제 효과를 보이지 않았다. PTP1B에 대해 뛰어난 억제활성을 보인 icaritin과 icariside II는 효소 반응 속도 연구를 통해 *k_i* 값은 각각 11.41 및 11.66 μM이며, 억제 유형은 모두 비경쟁적으로 나타났다. 분자 도킹 시뮬레이션에서 icaritin의 수산기가 PTP1B의 ASN193 잔기와 하나의 수소결합을 생성하여 -6.24 kcal/mol의 결합 에너지를 보였고, icariside II는 α-L-rhamnose 잔기의 수산기가 GLU276 잔기와 4개의 수소결합을 생성하여 -8.77 kcal/mol의 결합에너지를 보였다. 이 결과를 통해 icaritin과 icariside II가 PTP1B의 알로스테릭 자리에 결합함으로써 비경쟁적인 억제 활성을 보이는 것을 설명할 수 있다. BACE1 억제에서 icaritin과 icariside II가 IC₅₀ 35.90 ± 5.12 그리고 38.34 ± 2.65로 비슷한 활성을 보였으며, icariin은 79.02 ± 5.13의 IC₅₀ 값을 보였다. 또한, 분자 도킹 시뮬레이션에서 icaritin의 수산기가 catalytic 부위의 ASP228 잔기와 수소결합을 하고, icariside II는 catalytic 및 allosteric 부위에 모두 결합하므로 각각 경쟁적 및 혼합형 저해제로 보여진다. 반면에, AChE 억제에는 icariin, icaritin, epimedin A, epimedin B와 epimedin C가 뛰어난 효과를 보였다. AChE에 대한 억제 활성을 보인 화합물들은 효소 반응 속도 연구를 통해 모두 비경쟁적으로 AChE를 억제한다는 것을 알 수 있다. 분자 도킹 시뮬레이션 결과는 각 화합물이 AChE의 알로스테릭 조절에 관여하는 아미노산 잔기인 TYR70, ASP72, TYR121, TRP279 및 TYR334와 결합함으로써 비경쟁적으로 억제하는 것을 입증했다. 실험 결과와 화합물 구조를 비교 분석한 결과, prenylated flavonol의 C-3 및 C-7 위치에 당이 결합된 화합물이 AChE 저해에 좋은 활성을 보였다. 결론적으로, icaritin과 icariside II와 같은 icariin의 대사산물이 PTP1B 및 BACE1 억제에 뛰어난 활성을 나타냈으며, AChE 억제 효과에서는 주로 prenylated flavonol glycoside인 icariin, epimedin A, epimedin B 및 epimedin C가 가장 뛰어난 효과를 보였다. 이러한 결과는 효소 반응 속도 연구와 분자 도킹 시뮬레이션을 통해 증명할 수 있다. 따라서, 음양곽과 그 구성성분은 항당뇨 및 항알츠하이머 질병에 효과를 보이므로 당뇨병과 알츠하이머의 예방과 치료를 위한 전략으로의 가능성을 제시한다.

I. Introduction

Diabetes mellitus (DM) is considered as one of the foremost challenges of the twenty-first century characterized by group of metabolic disorders of heterogeneous etiology, and is augmented by hyperglycemia resulting from defects in insulin action and secretion. The chronic hyperglycemia of DM is involved in long-term damage, dysfunction, and failure of various organs, especially the eyes, kidneys, nerves, heart and blood vessels. It is occurred by insulin deficiency, often combined with insulin resistance (Gavin et al., 1997). DM is prevalent throughout the world and its incidence is rapidly increasing in most of countries (Parthasarathy et al., 2009). Insulin resistance, which is one of the hallmarks of DM, is occurred by disequilibrium in auto-phosphorylation of insulin receptor (IR) and activity of tyrosine kinase. Protein tyrosine phosphatase 1B (PTP1B) can interact with the activated IR, as well as insulin receptor substrate (IRS) proteins, and dephosphorylate the tyrosine residues of IR and IRS proteins (Kwon et al., 2008). PTP1B has been suggested as a negative regulator of the insulin metabolism *in vitro*. Regulation of insulin metabolic pathway by PTP1B has been exhibited in cell lines derived from both liver and muscle, in which it was shown to inhibit the insulin signaling pathway and the insulin-stimulated glycogen synthesis (Johnson et al., 2002). Massive research involving genetics and molecular approaches have been conducted which demonstrated that the overexpression of PTP1B resulted in states of insulin resistance (Elchebly et al., 1999; Liu et al., 2015). Therefore, inhibitors of PTP1B have been expected to prevent and treat DM and might act as promising insulin-sensitive drug target. In addition, the other method of the therapeutic approaches for decreasing postprandial hyperglycemia is to prevent absorption of carbohydrates after food uptake. Polysaccharide complexes are

hydrolyzed to dextrin or oligosaccharides by amylase and are further hydrolyzed to glucose by α -glucosidase before being absorbed into the epithelium of intestine and entering blood circulation (Shobana et al., 2009; Choi et al., 2010). α -Glucosidase is one of the group of enzymes, which is an exo-type α -glucosidic *O*-linkage-hydrolases releasing D-glucose from the non-reducing end side of substrate (Chiba, 1997). The α -glucosidase inhibitors (AGI) such as acarbose, miglitol and voglibose are generally used to treat diabetic patients, which delay the absorption of carbohydrates from the small intestine. Thus, AGIs have a decreasing effect on postprandial blood glucose and insulin levels (Van de laar et al., 2005). However, these AGIs are involved in unfavorable side effects, including liver toxicity, abdominal cramping, flatulence and diarrhea (Etxeberria et al., 2012). It is of great interest and reasons why the natural AGIs are preferred, having no unwanted adverse effects, are needed for treatment of DM. Therefore, pharmacological interventions aimed at preventive and therapeutic inhibition of α -glucosidase enzyme could be a potential strategy for the treatment of diabetes.

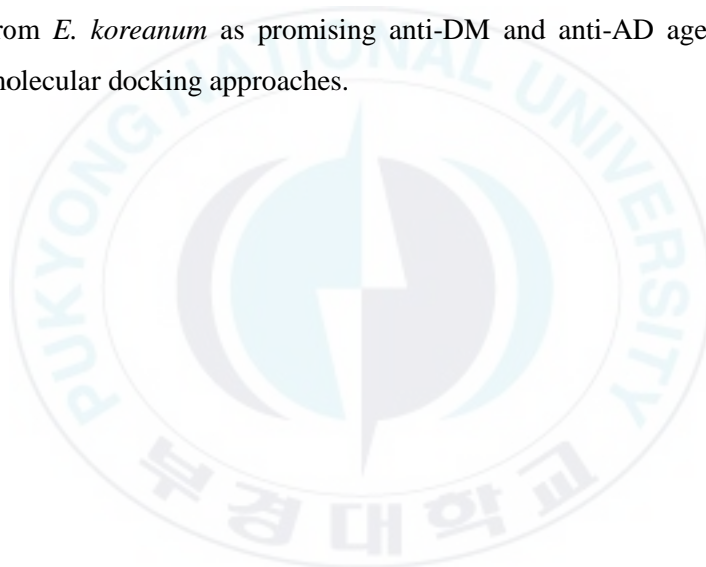
Alzheimer's disease (AD), the most common cause of dementia in the elderly, is a progressive neurodegenerative disease. It is characterized clinically by a gradual decrease of cognitive functions showing as memory loss and changes of behavior and personality (Chen et al., 2016). In addition, AD is pathologically featured by the presence of extracellular senile plaques and intracellular neurofibrillary tangles, loss of extensive neuronal and decrease in cholinergic transmission. Notably, the decline of memory and cognitive showed in AD patients correlates better with the synaptic pathology than either plaques or tangles, thus, synaptic dysfunction is probably the most significant factor causing to the early stages of memory loss (Scheltens and Feldman, 2003; Dickson et al., 1995). One of the targets of interest in treatment of AD is β -site amyloid precursor protein cleaving enzyme 1 (BACE1). BACE1 is associated with the primary and rate-limiting step of Amyloid- β peptides (A β) formation from amyloid precursor protein (APP)

(Jung et al., 2015). The accumulation of amyloid plaques is the important characteristic feature of AD, and investigation in the late 1980s identified the main plaque protein as the A β peptide. Once AD advances the cognitive defect caused by neuronal damage cannot be reversed, even after A β levels in the brain are depressed by immunotherapy (Gandy, 2011). Increased BACE1 activity resulting in increased A β production might be involved in treatment of patients with AD (Yang et al., 2003). Therefore, inhibitory activity of BACE1 is considered to be a factor to prevent A β accumulation. Another target of focusing on biological and pharmacological research for treatment of AD is cholinesterase (ChE) inhibitors. There are two ChEs, which are acetylcholinesterase (AChE) and butyrylcholinesterase (BChE). AChE is a specific ChE, hydrolyzing generally cholinesters, and featured by high concentrations in brain, neurons and red blood cells. The other type, called BChE, is a non-specific ChE (also called as “pseudo”-ChE) hydrolyzing other esters as well as cholinesters, and exist in blood serum, pancreas, liver, and central nervous system. Activity of acetylcholine (ACh) in the brain is terminated by the hydrolytic action of ChEs. The ChE inhibitors (ChEI) improve the activity of cholinergic neurons in the brain. All ChEIs presently allowed for treatment of AD inhibit AChE and to a diverse degree BChE in the brain (Rao et al., 2007). In healthy human brain, AChE predominates over BChE; however, the BChE likely has been previously undervalued (Li et al., 2000). AChE is localized mainly to neurons; BChE is involved mainly in the glial cells, as well as to endothelial cells and neurons (Darvesh et al., 2003). In addition, BChE acts as co-regulator of AChE, and is regarded as minor regulator of ACh levels in brain. However, levels of BChE are increased or unchanged in patients of AD, while AChE levels are decreased with changes becoming more pronounced during the disease course (Nordberg et al., 2013). Thus, inhibition of ChEs is considered to play an important role for prevent and treatment of AD.

Epimedii Herba (EH), also called as “Yin Yang Huo” or Horny Goat Weed, has been

used in traditional Chinese medicine (TCM) to treat impotence, infertility in woman, dysuria, rheumatic arthritis, geriatric depression, angina pectoris and so on (Nakashima et al., 2016; Chen et al., 2015). There are several species of the EH which belong to the same family of Berberidaceae, including *Epimedium brevicornum* Maxim. (Yin Yang Huo), *Epimedium koreanum* Nakai. (Korean Yin Yang Huo), *Epimedium grandiflorum* Morr. (Chang Ju Yin Yang Huo), *Epimedium sagittatum* (Sieb. et Zucc.) Maxim. (Jian Ye Yin Yang Huo), *Epimedium wushanense* T.S. Ying. (Wu Shan Yin Yang Huo) etc (Ma et al., 2011). The Chinese name of Yin Yang Huo came from the improved sexual function of sheep/goats. It has been identified for centuries that when *Epimedium* species plants consumed by sheep/goats, their frequency of coitus found to be increased. In addition, *Epimedium* plants are also called as "nine leaves on three stems" (San Zhi Jiu Ye Cao) in China, owing to the special characteristics of the aerial parts of *Epimedium* species, because every *Epimedium* plant has only three stems, and only three leaves on each stem (Wu et al., 2003). The aerial parts of *E. koreanum* Nakai are widely used in traditional Chinese and Korean herbal medicine (Oh et al., 2004). A wide range of pharmacological and biological activities of *E. koreanum* Nakai have been reported. The extract of *E. koreanum* has described as anti-diabetic (Oh et al., 2013), regulating sexual behavior (Makarova et al., 2007; Kang et al., 2012), and antiviral activity (Cho et al., 2012). In addition, *E. koreanum* contains a number of constituents including icariin, icarisode II, icaritin, epimedeside A-E, epimedin A-C, ikarisoside A-E, syringaresinol and icariresinol, which are flavonoid glycoside or lignan (Keum et al., 2014; Li et al., 1998; Li et al., 1995). The ability of icariin, the major component of *E. koreanum*, have been reported as anti-hepatotoxic (Lee et al., 1995), anti-tumor and anti-inflammatory agent (Zhou et al., 2011). Furthermore, other studies reported icariin bio-activities as vasodilation (Xu and Huang, 2007), improving dysfunction in spinal cord injury (Tohda and Nagata, 2012; Zhang et al., 2014), amelioration of diabetic retinopathy (Xin et al., 2012), and neuroprotective effects (Chen et al., 2016). Moreover, icarisode II has the potency of anti-

tumor (Lin et al., 1999), anti-hepatotoxic activity (Cho et al., 1995) and attenuation of streptozotocin-induced cognitive deficits (Yin et al., 2016). In addition, icaritin was reported as anti-cancer (Huang et al., 2007; Guo et al., 2011) and neuroprotective candidate (Wang et al., 2007). In another investigation by Zhang et al. (2013) reported that epimediphine has anti-AChE inhibitory activity. Despite the wide pharmacological potential of *E. koreanum*, there has been no systematic investigation which offers the possibility of developing personalized anti-DM and anti-AD drug candidates from *E. koreanum*. Therefore, this study proposes a prospective strategy for the development of compounds from *E. koreanum* as promising anti-DM and anti-AD agents by enzyme kinetics and molecular docking approaches.



II. Materials and methods

1. Plant materials

The aerial parts of *Epimedium koreanum* were collected from the Medicinal Herb Garden, Seoul, Korea, in November 2008 and confirmed by Professor Jinwoong Kim at College of Pharmacy, Seoul National University. A voucher specimen (no. 20081105) was deposited in the authorized laboratory.

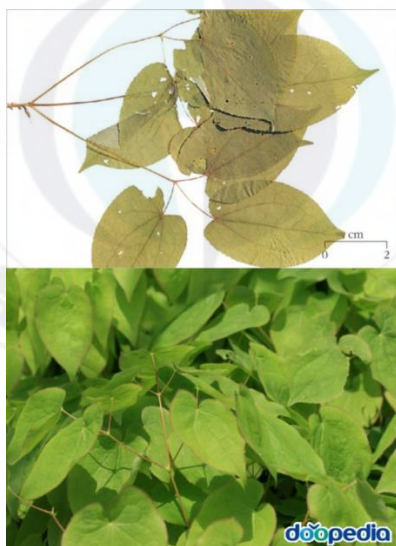


Figure 1. *Epimedium koreanum* Nakai (Korean Yin Yang Huo).

2. General experimental procedures

The $^1\text{H-NMR}$ and $^{13}\text{C-NMR}$ spectra were measured using a JEOL JNM ECP-400 (Japan) spectrometer at 400 and 100 MHz, respectively, in dimethylsulfoxide (DMSO-d_6) and chloroform (CDCl_3), and the EI-MS was determined by a JEOL JMS-700 spectrometer (Japan). The ultraviolet (UV) lamp (Model ENF-240C, Spectroline, USA) with built in both of 245 nm and 365 nm UV light was used to search spots on the thin layer chromatography (TLC) plates. The bioassays including PTP1B, α -glucosidase, AChE and BChE were conducted using a microplate reader spectrophotometer (Molecular Devices, VERSA max, CA, USA), and BACE1 was conducted using a microplate spectrofluorometer (Gemini XPS, Molecular Devices, Sunnyvale, CA, USA). Column chromatography was conducted using silica (Si) gel 60 (70–230 mesh, Merck, Darmstadt, Germany), Sephadex LH-20 (bead size 25–100 μm , Merck, Germany) and LiChroprep RP-18 (40–63 μm , Merck, Germany). All thin layer chromatography (TLC) were carried out using pre-coated Kieselgel 60 F_{254} plates (20 cm \times 20 cm, 0.25 mm, Merck) and RP-18 F_{254} s plates (5 \times 10 cm, Merck), using 50 % H_2SO_4 as a spray reagent. Solvents used in extraction, fractionation and column chromatography were or reagent grade, and were purchased from commercial sources.

3. Chemicals and Reagents

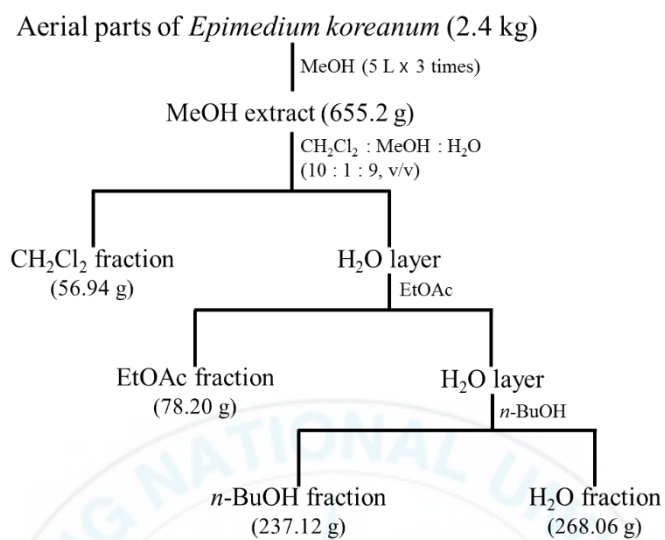
p-Nitrophenyl phosphate (*p*NPP), ethylenediamine tetra acetic acid (EDTA), yeast α -glucosidase, *p*-nitrophenyl α -D-glucopyranoside (*p*NPG), acarbose, electric-eel AChE (EC3.1.1.7), horse-serum BChE (EC 3.1.1.8), acetylthiocholine iodide (ATCh), butyrylthiocholine chloride (BTCh) and 5-5'-dithiobis [2-nitrobenzoic acid] (DTNB)

were purchased from Sigma-Aldrich Co. (St. Louis, MO, USA). PTP1B (human recombinant) was purchased from Biomol International LP (Plymouth Meeting, PA, USA), and dithiothreitol (DTT) was purchased from Bio-Rad Laboratories (Hercules, CA, USA). BACE1 FRET assay kit (β -secretase) was purchased from the Pan Vera Co. (Madison, WI, USA). Magnolol was purchased from Sigma-Aldrich Co. (St. Louis, UT, USA), (-)-syringaresinol was offered from Professor Byung Sun Min at College of Pharmacy, Catholic University of Daegu, and icariin, icaritin and icariside II were offered from Amorepacific Co., and epimedin A, epimedin B and epimedin C were purchased from the Roehen pharma Co. Ltd. (Rd Dong Lu, SH, China).

4. Experiment methods

4-1. Extraction and fractionation

The dried aerial parts of *E. koreanum* (2.4 kg) were extracted with MeOH (5 L \times 3times) for 3 hours under reflux. After filtration, total filtrate was then concentrated to dryness *in vacuo* at 40°C to give a MeOH extract (655.2 g). Then the MeOH extract was suspended in H₂O and successively partitioned with dichloromethane (CH₂Cl₂), ethyl acetate (EtOAc) and *n*-butanol (*n*-BuOH) to yield CH₂Cl₂ (56.94 g), EtOAc (78.20 g), *n*-BuOH (237.12 g) and H₂O (268.06 g) fractions.

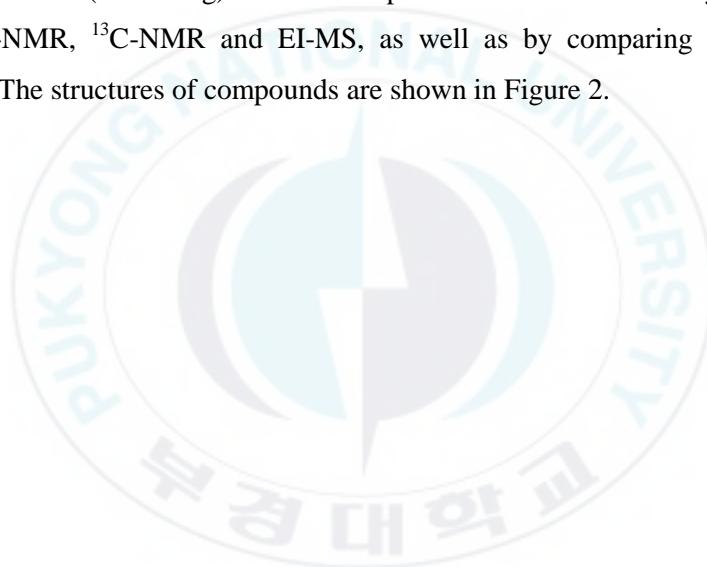


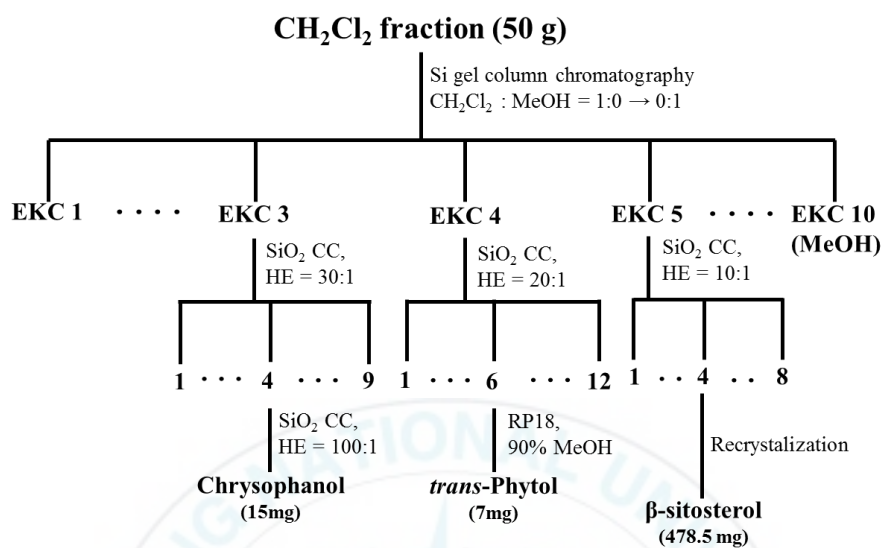
Scheme 1. Extraction and fractionation of aerial parts of *E. koreanum*.

4-2. Isolation of compounds

4-2-1. Isolation of compounds from the CH₂Cl₂ fraction

CH₂Cl₂ fraction (50 g) was chromatographed on Si gel column chromatography (CC) with CH₂Cl₂-MeOH (1:0 to 0:1) solvent system to give 10 subfractions (EKC 1-10). EKC 3 was chromatographed on Si gel column with *n*-hexane-EtOAc (30:1) to yield chrysophanol (15 mg). EKC 4 was subjected to Si gel CC using *n*-hexane-EtOAc (20:1) to obtain *trans*-phytol (7 mg). Successive recrystallization of EKC54 using MeOH yielded β-sitosterol (478.5 mg). These compounds were identified by spectroscopy including ¹H-NMR, ¹³C-NMR and EI-MS, as well as by comparing with published spectral data. The structures of compounds are shown in Figure 2.



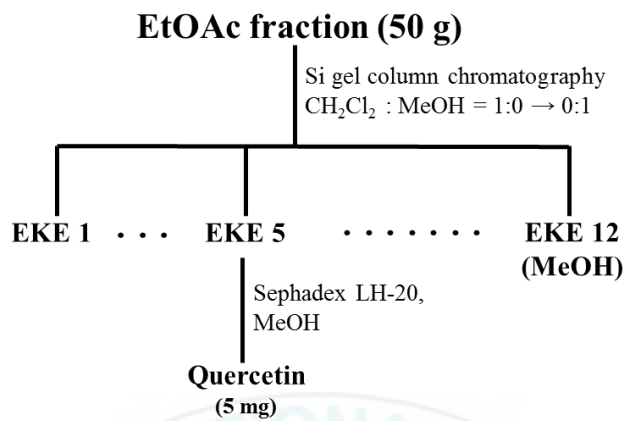


Scheme 2. Isolation of compounds from the CH₂Cl₂ fraction of *E. koreanum*.

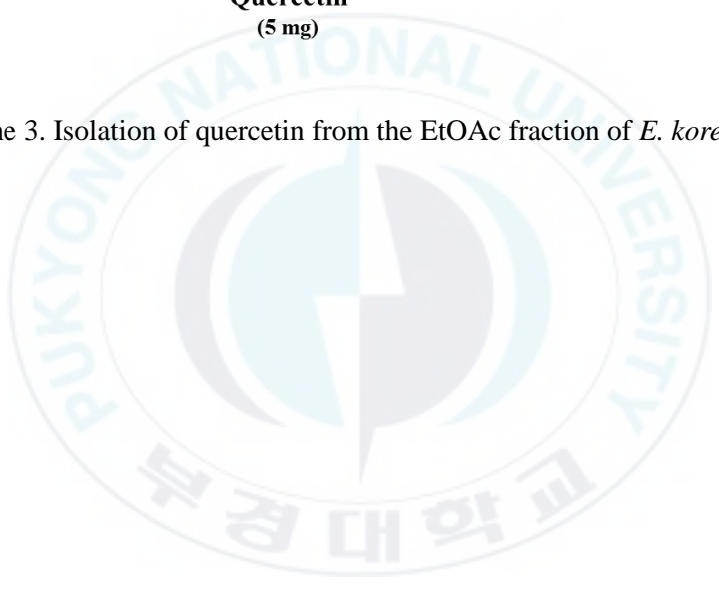
4-2-2. Isolation of quercetin from the EtOAc fraction

EtOAc fraction (50 g) was subjected to Si gel CC with CH_2Cl_2 -MeOH (1:0 to 0:1) solvent system to give 12 subfractions (EKE 1-12). EKE 5 was chromatographed on Sephadex LH-20 with MeOH and Si gel CC to yield quercetin (5 mg). Quercetin was identified by spectroscopy including ^1H - and ^{13}C -NMR by comparing with published spectral data. The structure is shown in Figure 2.





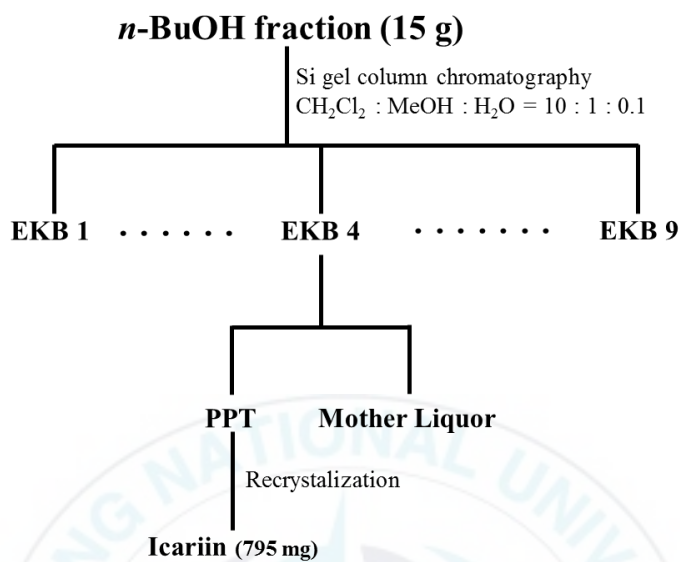
Scheme 3. Isolation of quercetin from the EtOAc fraction of *E. koreanum*.



4-2-3. Isolation of icariin from the *n*-BuOH fraction

n-BuOH fraction (15 g) was subjected to CC on Si gel with CH₂Cl₂:MeOH:H₂O (10:1:0.1) solvent system to collect 8 fractions (EKB 1-9). Recrystallization of EKB 4 using MeOH yielded icariin (795 mg). Icariin was identified by comparing with the R_f value on TLC. The structure is shown in Figure 2.





Scheme 4. Isolation of icariin from the *n*-BuOH fraction of *E. koreanum*.

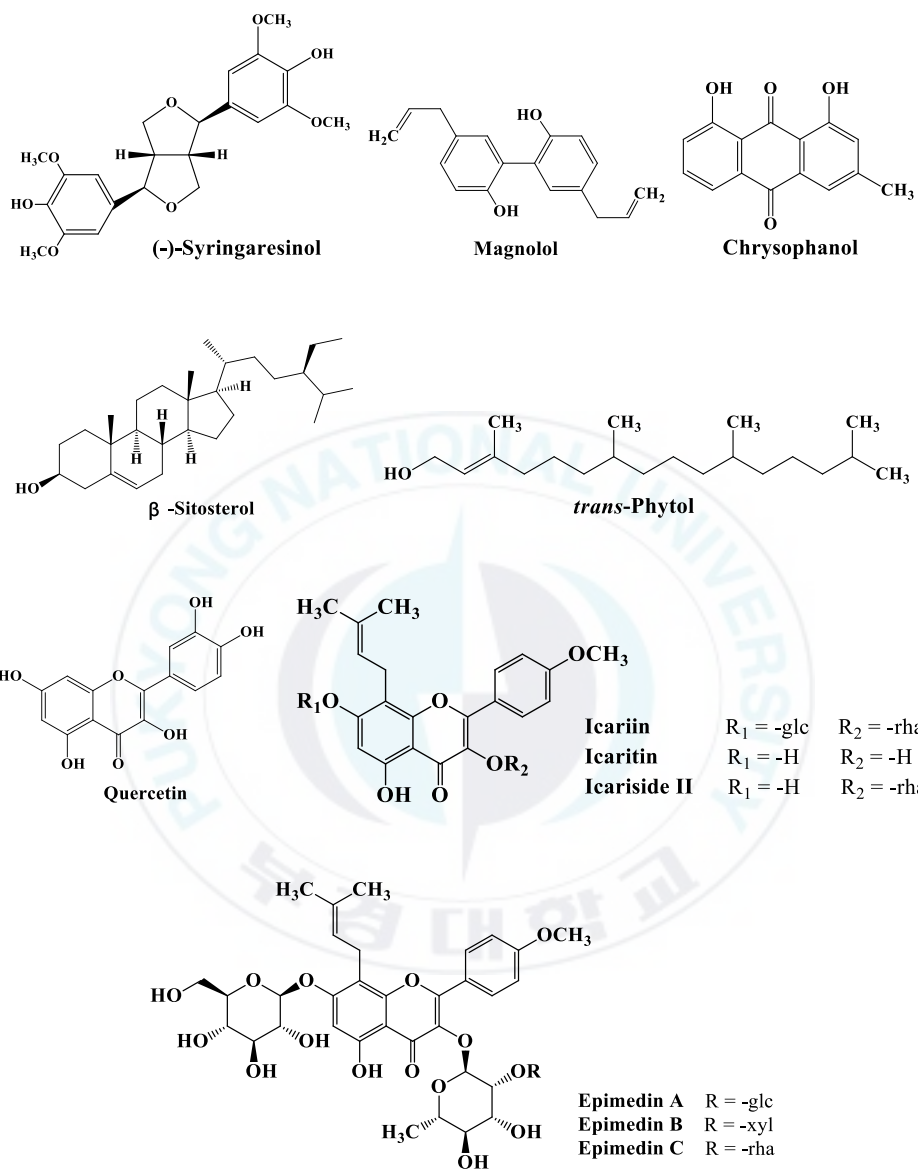


Figure 2. Chemical structures of compounds.

4-3. Anti-diabetic experiments

4-3-1. PTP1B inhibitory assay

The PTP1B (human recombinant) inhibitory activities of the aerial parts of *E. koreanum* and its constituents were evaluated using *p*NPP as substrate (Cui et al., 2006). To each well of 96-well-plate (final volume 100 μ L), PTP1B enzyme diluted using PTP1B reaction buffer containing 50 mM citrate (pH 6.0), 0.1 M NaCl, 1 mM EDTA, and 1 mM DTT was added with or without a test sample. Then, 50 μ L of 2 mM *p*NPP dissolving in PTP1B reaction buffer was added. After incubation at 37°C for 20 min in the dark, the reaction was terminated with the addition of 10 M NaOH. The amount of *p*-nitrophenylate produced by enzymatic dephosphorylation of *p*NPP was determined by measuring the absorbance at 405 nm using a microplate reader spectrophotometer (Molecular Devices, VERSA max CA, USA). The non-enzymatic dephosphorylation of *p*NPP was corrected by measuring the increase in absorbance at 405 nm obtained in the absence of PTP1B enzyme. Ursolic acid was used as a positive control. The inhibition (%) was calculated as $\{(A_C - A_S) / A_C\} \times 100$, where A_C is the absorbance of the control and A_S , the absorbance of the sample. The half maximal inhibitory concentration (IC_{50}) is expressed as the mean \pm S.E.M. of triplicate experiments.

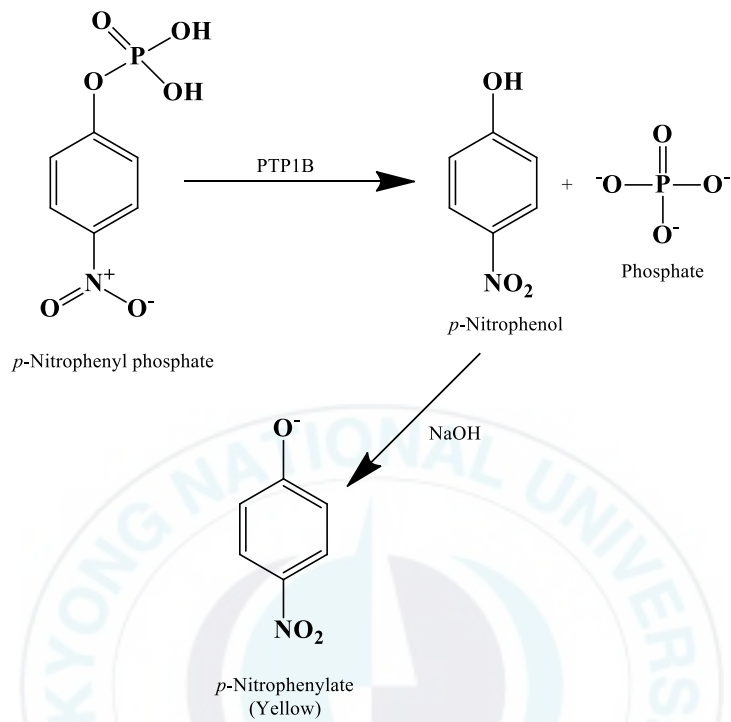


Figure 3. Enzymatic principle of the PTP1B inhibitory assay.

4-3-2. α -Glucosidase Inhibitory assay

The α -glucosidase enzyme assay was carried out spectrophotometrically using the reported procedure (Li et al., 2005). Briefly, a total of 60 μ L of reaction mixture containing 20 μ L of 100 mM phosphate buffer (pH 6.8), 20 μ L of 2.5 mM *p*NPG, and 20 μ L of the sample (final concentration ranging from 20 to 300 μ M dissolved in 10% DMSO) was added to each well. After incubation at 37 $^{\circ}$ C for 5 min in the dark, 20 μ L α -glucosidase (0.2 U/mL) in 10 mM phosphate buffer (pH 6.8) was added. The plate was again incubated at 37 $^{\circ}$ C for 15 min in the dark, and then 80 μ L of 0.2 M sodium carbonate solution was added to stop the reaction. The absorbance was immediately recorded at 405 nm using a microplate reader spectrophotometer (Molecular Devices, VERSA max CA, USA). The control was the same reaction mixture containing an equivalent volume of phosphate buffer instead of the sample solution. Acarbose dissolved in 10% DMSO was used as a positive control. The inhibition (%) was calculated as $\{(A_C - A_S) / A_C\} \times 100$, where A_C is the absorbance of the control and A_S , the absorbance of the sample. The IC_{50} is expressed as the mean \pm S.E.M. of triplicate experiments.

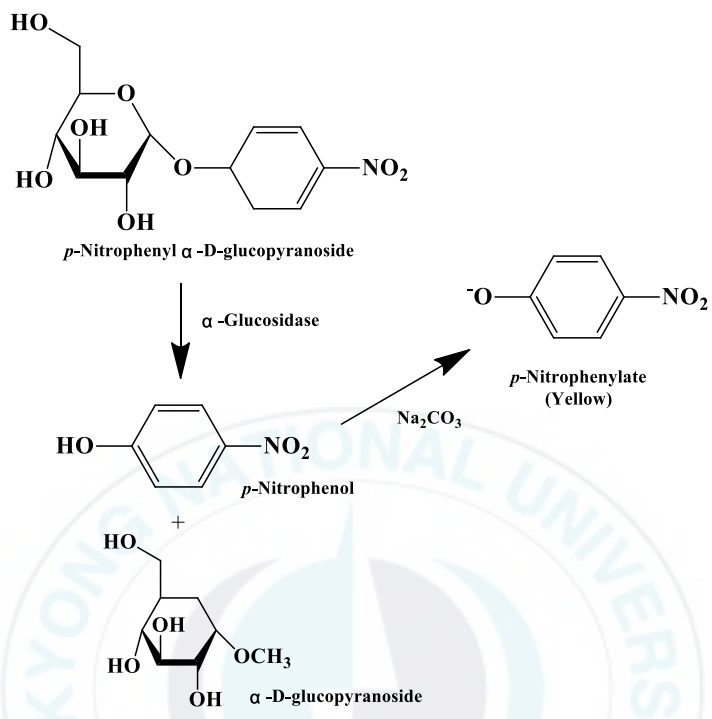


Figure 4. Enzymatic principle of the α -glucosidase inhibitory assay.

4-3-3. Enzyme kinetic analysis with PTP1B

In order to determine the inhibition mechanism, two kinetic methods such as Lineweaver-Burk and Dixon plots were complementarily used (Lineweaver and Burk, 1934; Dixon, 1953; Cornish-Bowden, 1974). Each enzymatic inhibition at various concentrations of test samples was evaluated by monitoring the effect of different concentration of the substrate in Dixon plots (single reciprocal plot). Dixon plots for inhibition of PTP1B were obtained in the presence of different concentrations of *p*NPP. Using Lineweaver-Burk plots (double reciprocal plot), the inhibition mode of compounds were determined at various concentrations of *p*NPP with different concentrations of compounds. The enzymatic procedures consisted of the same aforementioned PTP1B assay methods. The types of inhibition were investigated by interpreting the Dixon plots, in which the value of the x-axis indicating K_i .

4-4. Anti-Alzheimer's disease experiments

4-4-1. BACE1 inhibitory assay

The assay was carried out according to the supplied manual with selected modifications. Briefly, a mixture of 10 μL of assay buffer (50 mM sodium acetate, pH4.5), 10 μL of BACE1 (1.0 U/mL), 10 μL of substrate (750 nM Rh-EVNLDAEFK-Quencher in 50 mM, ammonium bicarbonate) and 10 μL of the tested samples (final concentration: 300 $\mu\text{g/mL}$ for the extract and each fractions, and 300 μM for the compounds) dissolved in 10 % DMSO was incubated at room temperature for 1 hour in the dark. The proteolysis of two fluorophores (Rh-EVNLDAEFK-Quencher) by BACE1 was monitored by the formation of the fluorescent donor Rh-EVNL (530-545 nm, excitation; 570-590 nm, emission), the abundance of which was determined by measuring the increase in fluorescence excited at 545 nm and recorded at 585 nm. Fluorescence was measured with a microplate spectrofluorometer (Gemini XTS, Molecular Devices, Sunnvale, CA, USA). Quercetin dissolved in 10% DMSO was used as a positive control. The percent inhibition (%) was obtained by the following equation: inhibition % = $\{1 - (S_{60} - S_0) / (C_{60} - C_0)\} \times 100$, where S_{60} is the fluorescence of the tested samples (sample solution, substrate and enzyme) after 60 min incubation, S_0 is the initial fluorescence of the tested samples, C_{60} is the fluorescence of the control (buffer, substrate and enzyme) after 60 min incubation and C_0 is the initial fluorescence of the control. To allow for the quenching effect of the samples, the sample solution was added to a separate reaction mixture C, and any reduction in fluorescence by the sample was investigated. The IC_{50} is expressed as the mean \pm S.E.M. of triplicate experiments.

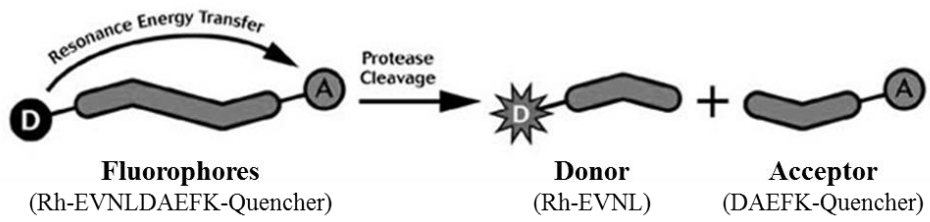


Figure 5. Enzymatic principle of BACE1 inhibitory assay.



4-4-2. AChE and BChE inhibitory assay

The inhibitory activities of the AChE and BChE were measured using the spectrophotometric method by Ellman et al. (1961). Essentially, acetylthiocholine iodide (ATCh) and butyrylthiocholine chloride (BTCh) were used as substrate to detect the inhibitions of AChE and BChE, respectively. All tested samples were dissolved in 10 % DMSO. Then, the reaction mixture contained: 20 μ L of tested sample solution (final concentration ranging from 1 to 300 μ M for compounds); 140 μ L of sodium phosphate buffer (pH 8.0); and 20 μ L of AChE or BChE solution, which were mixed and incubated for 15 min at room temperature. Reactions were started by adding 10 μ L of DTNB and 10 μ L of ATCh or BTCh. The hydrolysis of ATCh or BTCh was monitored by following the formation of the yellow 5-thio-2-nitrobenzoate, which formed by the reaction between DTNB and thiocholine, released by the enzymatic hydrolysis of ATCh or BTCh, at 412 nm. All reactions were performed in triplicate and recorded in 96-well microplate using a microplate reader spectrophotometer (Molecular Devices, VERSA max CA, USA). Berberine dissolved in 10% DMSO was used as a positive control. The inhibition (%) was calculated as $\{(A_C - A_S) / A_C\} \times 100$, where A_C is the absorbance of the control and A_S , the absorbance of the sample. The IC_{50} is expressed as the mean \pm S.E.M. of triplicate experiments.

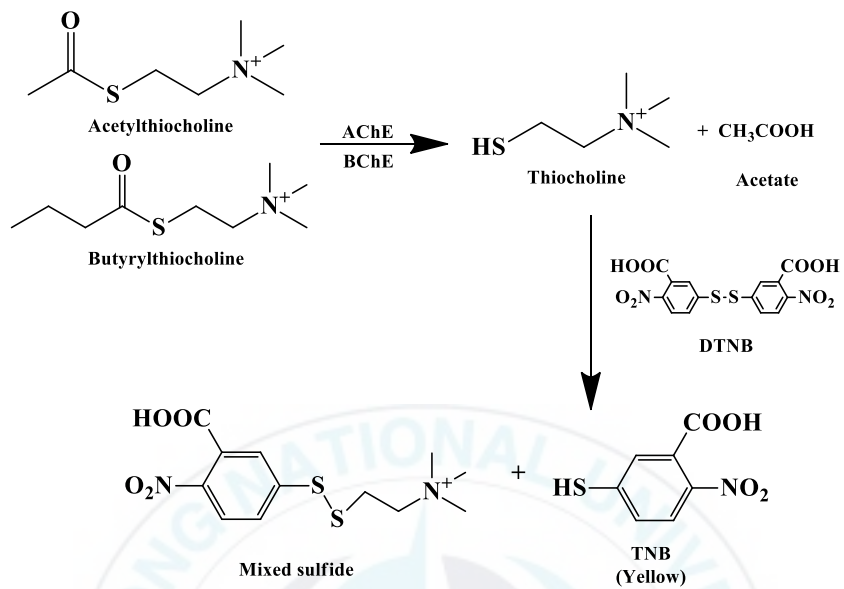


Figure 6. Enzymatic principle of ChEs inhibitory assay.

4-4-3. Enzyme kinetic analysis with AChE

In order to determine the inhibition mechanism, two kinetic methods such as Lineweaver-Burk and Dixon plots were complementarily used (Lineweaver and Burk, 1934; Dixon, 1953; Cornish-Bowden, 1974). Each enzymatic inhibition at various concentrations of test samples was evaluated by monitoring the effect of different concentration of the substrate in Dixon plots (single reciprocal plot). Dixon plots for inhibition of AChE were obtained in the presence of different concentrations of ATCh. Using Lineweaver-Burk plots (double reciprocal plot), the inhibition mode of compounds were determined at various concentrations of ATCh with different concentrations of compounds. The enzymatic procedures consisted of the same aforementioned AChE assay methods. The types of inhibition were investigated by interpreting the Dixon plots, in which the value of the x-axis indicating K_i .

4-5. Molecular docking simulation

4-5-1. Molecular docking simulation in PTP1B inhibition

X-ray crystallographic structure of PTP1B (PDB ID: 1T49), with its potent and selective inhibitor 3-(3,5-dibromo-4-hydroxy-benzoyl)-2-ethyl-benzofuran-6-sulfonic acid (4-sulfamoyl-phenyl)-amide was obtained from the RCSB Protein Data Bank (Bernstein et al., 1977; Berman et al., 2002) at resolution of 1.9 Å (Wisemann et al., 2004). The binding PTP1B inhibitor and water molecules were removed from the structure for the docking simulation using Accelrys Discovery Studio 4.1 (Accelrys, Inc. San Diego, CA, USA). The 3D structures of icaritin and icariside II were obtained from the PubChem Compound (NCBI), with compound CIDs of 5318980 and 44587252, respectively. Automated docking simulation was performed using AutoDock Tool (ADT) to assess the appropriate binding orientations and conformations of the PTP1B with the different compounds. A Lamarckian genetic algorithm method implemented in AutoDock 4.2 was employed. For docking calculations, Gasteiger charges were added by default, the rotatable bonds were set by the ADTs, and all torsions were allowed to rotate. The grid maps were generated by the Autogrid program where the grid box size of 80 × 80 × 80 had a default spacing of 0.375 Å. The X, Y, Z center were 51, 19.034 and 14.048. The docking protocol for rigid and flexible ligand docking consisted of 10 independent Genetic Algorithms (GA), while other parameters were used as defaults of the ADTs. The binding aspect of PTP1B residues and their corresponding binding affinity score were regarded as the best molecular interaction. The results were analyzed using UCSF Chimera (Pettersen et al., 2004), while the hydrogen bonds and Van der Waals interaction residues were visualized by Ligplot 1.4.5.

4-5-2. Molecular docking simulation in BACE1 inhibition

X-ray crystallographic structure of BACE1 (PDB ID: 2WJO), with its potent inhibitor

2-amino-3-((1R)-1-cyclohexyl-2-[(cyclohexylcarbonyl)amino]ethyl)-6-phenoxyquinazolin-3-ium (QUD) was obtained from the RCSB Protein Data Bank (Bernstein et al., 1977; Berman et al., 2002) at resolution of 2.5 Å (Nicholls et al., 2010). The binding BACE1 inhibitor and water molecules were removed from the structure for the docking simulation using Accelrys Discovery Studio 4.1 (Accelrys, Inc. San Diego, CA, USA). The 3D structures of icaritin and icariside II were obtained from the PubChem Compound (NCBI), with compound CIDs of 5318980 and 44587252, respectively. Automated docking simulation was performed using Autodock tools (ADT) to assess the appropriate binding orientations and conformations of the BACE1 with the different compounds. A Lamarckian genetic algorithm method implemented in AutoDock 4.2 was employed. For docking calculations, Gasteiger charges were added by default, the rotatable bonds were set by the ADTs, and all torsions were allowed to rotate. The grid maps were generated by the Autogrid program where the grid box size of 80 × 80 × 80 had a default spacing of 0.375 Å. The X, Y, Z center were 18.317, 37.606 and 47.577. The docking protocol for rigid and flexible ligand docking consisted of 10 independent Genetic Algorithms (GA), while other parameters were used as defaults of the ADTs. The binding aspect of BACE1 residues and their corresponding binding affinity score were regarded as the best molecular interaction. The results were analyzed using UCSF Chimera (Pettersen et al., 2004), while the hydrogen bonds and Van der Waals interaction residues were visualized by Ligplot 1.4.5.

4-5-3. Molecular docking simulation in AChE inhibition

X-ray crystallographic structure of AChE (PDB ID: 1EVE), with its potent and selective inhibitor 1-benzyl-4[(5,6-dimethoxy-1-indanon-2-yl)methyl]piperidine (E2020) was obtained from the RCSB Protein Data Bank (Bernstein et al., 1977; Berman et al., 2002) website at resolution of 2.5 Å (Kryger et al., 1999). The reported AChE inhibitor E2020 and water molecules were removed from the structure for the docking simulation

using Accelrys Discovery Studio 4.1 (Accelrys, Inc. San Diego, CA, USA). The 3D structures of icariin, icaritin, epimedin A, epimedin B and epimedin C were obtained from the PubChem Compound (NCBI), with compound CIDs of 5318997, 5318980, 92043273, 5748393 and 5738394, respectively. Automated docking simulation was performed using ADT to assess the appropriate binding orientations and conformations of the AChE with the different compounds. A Lamarckian genetic algorithm method implemented in AutoDock 4.2 was employed. For docking calculations, Gasteiger charges were added by default, the rotatable bonds were set by the ADT, and all torsions were allowed to rotate. The grid maps were generated by the Autogrid program where the grid box size of $40 \times 40 \times 40$ had a default spacing of 0.375 \AA . The X, Y, Z center were 4.8, 64.426 and 66.718. The docking protocol for rigid and flexible ligand docking consisted of 10 independent GA, while other parameters were used as defaults of the ADTs. The binding aspect of AChE residues and their corresponding binding affinity score were regarded as the best molecular interaction. The results were analyzed using UCSF Chimera (Pettersen et al., 2004), while the hydrogen bonds and Van der Waals interaction residues were visualized by Ligplot 1.4.5.

5. Statistical analysis

The data were evaluated using one-way ANOVA followed by Student's *t* test (Systat Inc., Evanston, IL, USA). All results were expressed as means \pm SEM. *P* values < 0.01 were considered to indicate significance.

III. Results

1. Anti-diabetic activity

1-1. PTP1B and α -glucosidase inhibitory activities of the MeOH extract and its solvent soluble fractions from aerial parts of *E. koreanum*

In order to determine the ant-diabetic potential of aerial parts of *E. koreanum*, MeOH extract and its soluble fractions were evaluated for inhibitory activities against PTP1B and α -glucosidase. As represented in Table 1, CH₂Cl₂ fraction showed strong PTP1B inhibition at the tested concentrations displaying IC₅₀ value of 3.51 ± 0.05 $\mu\text{g/mL}$ compared to ursolic acid, positive control with an IC₅₀ value of 5.54 $\mu\text{g/mL}$. As shown in Figure 7, the MeOH extract of aerial parts of *E. koreanum* demonstrated significant PTP1B inhibitory activity in a dose dependent manner with IC₅₀ value of 18.83 ± 0.14 $\mu\text{g/mL}$. Moreover, EtOAc, *n*-BuOH and H₂O fractions exhibited moderate PTP1B inhibitory activities with IC₅₀ values of 27.09 ± 0.30 , 14.44 ± 0.68 , and 38.36 ± 1.29 $\mu\text{g/mL}$, respectively (Table 1).

The α -glucosidase inhibitory activity of MeOH extract and its fractions are shown in Table 1. Among the four solvent soluble fractions, the CH₂Cl₂ and EtOAc presented potent α -glucosidase inhibitory effects with IC₅₀ values of 47.69 ± 0.32 and 75.87 ± 0.38 $\mu\text{g/mL}$, respectively, compared to acarbose used as positive control representing IC₅₀ value of 87.83 ± 1.08 $\mu\text{g/mL}$. In contrast, the MeOH extract and other fractions (*n*-BuOH

and H₂O) showed moderate α -glucosidase inhibitory activities with IC₅₀ values of 120.75 \pm 3.06, 138.90 \pm 0.02, and 310.01 \pm 1.29 μ g/mL, respectively (Table 1).



Table 1. Inhibitory activities of the MeOH extract and its fractions from *Epimedium koreanum* on PTP1B and α -glucosidase

Samples	Yields (g)	IC ₅₀ (μ g/mL) ^a	
		PTP1B	α -Glucosidase
MeOH extract	665.2	18.83 \pm 0.14	120.75 \pm 3.06
CH ₂ Cl ₂ fraction	56.94	3.51 \pm 0.05	47.69 \pm 0.32
EtOAc fraction	78.20	27.09 \pm 0.30	75.87 \pm 0.38
<i>n</i> -BuOH fraction	237.12	14.44 \pm 0.68	138.90 \pm 0.02
H ₂ O fraction	268.06	38.36 \pm 1.29	310.01 \pm 1.29
Ursolic acid ^b	-	5.54 \pm 0.13	
Acarbose ^b	-		87.83 \pm 1.08

^a The 50% inhibitory concentration (IC₅₀) values (μ g/mL) were calculated from a log dose inhibition curve and expressed as mean \pm S.E.M of triplicate experiments. ^b Used as positive control.

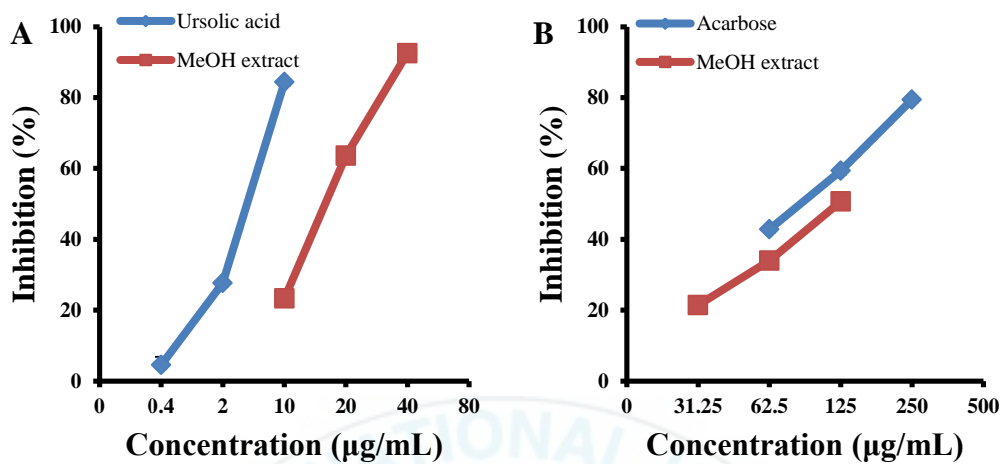


Figure 7. Inhibitory activities of the MeOH extract from *Epimedium koreanum* on (A) PTP1B, (B) α -glucosidase. All values are expressed as mean \pm S.E.M of triplicate experiments. Ursolic acid and acarbose were used as positive control.

1-2. PTP1B and α -glucosidase inhibitory activities of the compounds

In order to determine and identify the active compounds of *E. koreanum* responsible for the potent anti-diabetic activities, PTP1B and α -glucosidase inhibitory potential of compounds were evaluated. As shown in Table 2, icaritin and icariside II exhibited the most profound activities with IC_{50} values of 11.59 ± 1.39 and 9.94 ± 0.15 μ M, respectively, compared with ursolic acid ($IC_{50} = 8.24 \pm 0.03$ μ M). However, the rest of the compounds showed no inhibitory activity against PTP1B at tested concentrations (Table 2).

Among the tested compounds, icaritin and icariside II presented convincing effect against α -glucosidase showing IC_{50} values of 74.42 ± 0.01 and 106.59 ± 0.44 μ M compared with acarbose ($IC_{50} = 101.16 \pm 3.69$ μ M). In contrast, epimedin A, epimedin B and epimedin C showed moderate α -glucosidase inhibitory activities, following IC_{50} values of 444.09 ± 3.8 μ M, 451.78 ± 5.36 μ M and 403.87 ± 1.53 μ M, respectively. However, icariin, magnolol and (-)-syringaresinol exhibited no inhibitory effect under the tested concentrations.

Table 2. Inhibitory activities of compounds of *Epimedium koreanum* on PTP1B and α -glucosidase

Compounds	IC ₅₀ (μ M) ^a	
	PTP1B	α -Glucosidase
Icariin	> 300	> 300
Icaritin	11.59 \pm 1.39	74.42 \pm 0.01
Icariside II	9.94 \pm 0.15	106.59 \pm 0.44
Epimedin A	> 300	> 300
Epimedin B	> 300	> 300
Epimedin C	> 300	> 300
Magnolol	> 300	> 300
(-)-Syringaresinol	> 300	> 300
Ursolic acid ^b	8.24 \pm 0.03	
Acarbose ^b		101.16 \pm 3.69

^a The 50% inhibitory concentration (IC₅₀) values (μ M) were calculated from a log dose inhibition curve and expressed as mean \pm S.E.M of triplicate experiments. ^b Used as positive control.

1-3. Enzyme kinetic analysis of compounds with PTP1B

Since the results from PTP1B inhibitory activity demonstrated that tested compounds displayed two active compounds (icaritin and icariside II), these compounds were further analyzed to establish the correlation between compounds and substrate (*p*NPP) in PTP1B. The inhibition type and inhibition constant (K_i) of two compounds were determined using the Lineweaver-Burk and Dixon plots. Each line of inhibitors intersected at the y-intercept, indicating competitive-type inhibitor, while the lines passing through same point at the x-intercept, representing noncompetitive-type inhibitor, and the line intersected at the xy-side, showing mixed-type inhibitor in the Lineweaver-Burk plots. Therefore, icaritin and icariside II showed noncompetitive-type inhibition against PTP1B (Figure 8). In addition, the Dixon plot is an ordinary method for determining the enzyme inhibition type and the K_i value for an enzyme-inhibitor complex, where the value of the x-axis suggests K_i . As shown in Figure 8, the K_i values of icaritin and icariside II were 11.41 and 11.66 μ M, respectively.

Table 3. Enzyme kinetic analysis of compounds of *E. koreanum* with PTP1B

Test compounds	K_i (μM)^a	Inhibition type^b
Icaritin	11.41	Non-competitive
Icariside II	11.66	Non-competitive

^a Determined by the Dixon plot. ^b Determined by the Lineweaver-Burk plot.



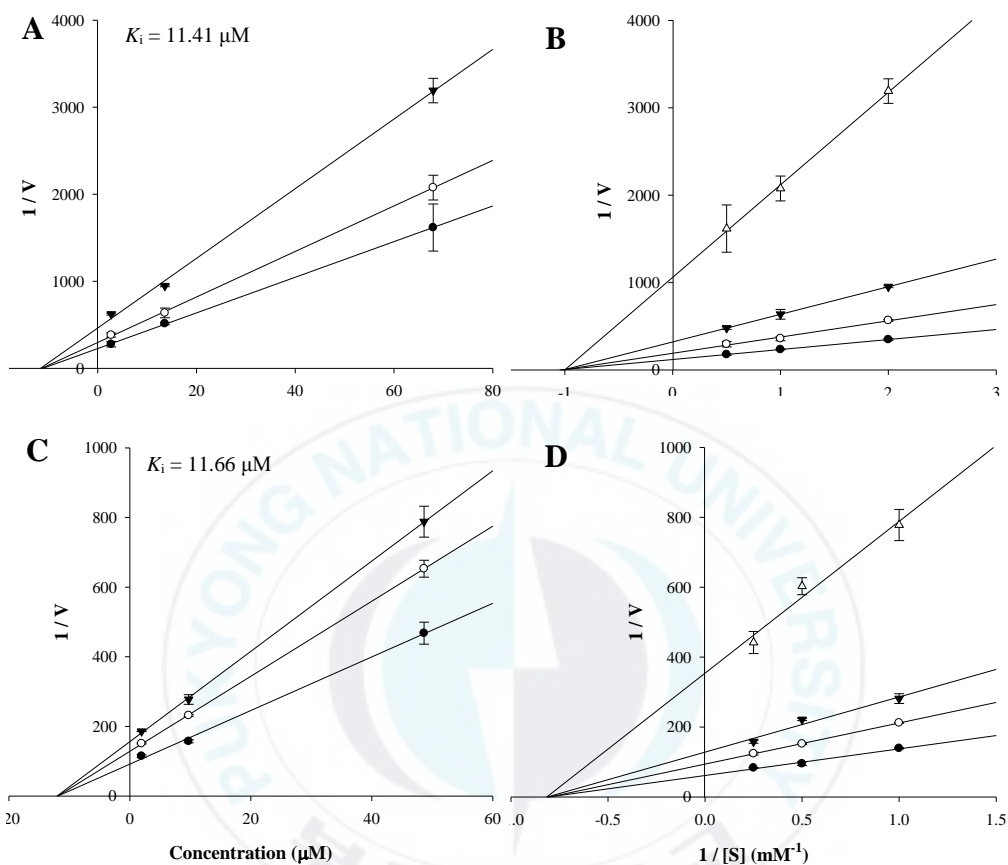


Figure 8. Dixon and Lineweaver-Burk plots of the inhibition of PTP1B by icaritin and icariside II. The results showed the effects of the presence of different concentrations of the substrate (2.0 mM (●), 1.0 mM (○) and 0.5 mM (▼) for (A) icaritin and 4.0 mM (●), 2.0 mM (○) and 1.0 mM (▼) for (C) icariside II) and the effect of the presence of different concentration of (B) icaritin (0 μM (●), 2.72 μM (○), 13.59 μM (▼) and 67.93 μM (Δ)) and (D) icariside II (0 μM (●), 1.94 μM (○), 9.73 μM (▼) and 48.64 μM (Δ)).

1-4. Molecular docking simulation in PTP1B inhibition

Molecular docking simulation study was performed to validate the mechanism of the interaction between compounds and the active site of PTP1B. In this study, the 3D docking of active compounds (icaritin and icariside II) were simulated, where 3-({5-[(N-acetyl-3-{4-[(carboxycarbonyl)(2-carboxyphenyl)amino]-1-naphthyl}-L-alanyl)amino]pentyl}oxy)-2-naphthoic acid (positive ligand of catalytic model of PTP1B, compound 23) and 3-(3,5-dibromo-4-hydroxy-benzoyl)-2-ethyl- benzofuran-6-sulfonic acid (4-sulfamoyl-phenyl)-amide (positive ligand of allosteric model, compound 2) were considered as the standard ligand to compare the orientation of the tested compounds. The docking analysis were conducted to validate structure-activity relationship of compounds with the obtained experimental data as well as used to evaluate the binding site-directed inhibition of PTP1B. The AutoDock 4.2 program uses a semi-empirical free energy force field to guess the binding complexes of protein-ligand of a known structure and the binding energies for bound state. The results of docking simulations of four compounds are shown in Table 4 and Figure 9. The PTP1B-icaritin complex showed – 6.24 kcal/mol of binding energy with one hydrogen bond interacting with residue ASN193. The nitrogen group of ASN193 was involved in the strong hydrogen bonding with the hydroxyl group (O2) of icaritin with bond distance of 2.69 Å. Moreover, hydrophobic interactions were also exhibited between SER187, ALA189, SER190, LEU192, PHE196, GLU276, GLY277 and PHE280. These hydrophobic interactions are important to intensify the protein-ligand interaction and for positioning of icaritin in the active pocket to inhibit PTP1B activity. The binding energy of PTP1B-icariside II complex was –8.77 kcal/mol with four hydrogen bonds interacting with GLU276. The oxygen groups of GLU276 residue were involved in the hydrogen bonding interaction with the hydroxyl groups (O3, O4 and O5) of icariside II with bond distance ranging from 2.59 to 3.13 Å. In addition, hydrophobic interactions were also observed between

SER187, ALA189, LEU192, ASN193, PHE196, LYS197, GLU200, GLY277, PHE280 and ILE281. These hydrophobic interactions provide further stability to the complex and help to fit thoroughly in the active pocket of PTP1B. Therefore, the hydrogen and hydrophobic interactions with PTP1B might be associated with the hydrolysis of substrate molecule. The molecular docking simulation result was corresponded well with the experimental data with respect to the PTP1B inhibitory activity of compounds.



Table 4. Binding site residues and docking scores of compounds in protein tyrosine phosphatase 1B (PTP1B) using AutoDock 4.2 program

Compounds	Binding energy ^a (kcal/mol)	No. of H-bond	H-bond interacting residues ^b	Van der Waals bond interacting residues ^c
Compound 23 ^d (catalytic inhibitor)	-11.23	11	TYR46, ASP48, ARG24, SER216, ALA217, ARG221, ARG254, GLN262	SER28, VAL49, LYS116, LYS120, CYS215, ILE219, GLY220, MET258, GLY259
Compound 2 ^d (allosteric inhibitor)	-10.98	2	ASN193, GLU276	PHE196, GLY277, PHE280, ILE281, MET282, LYS279, ALA189, LEU192
Icaritin	-6.24	1	ASN193	SER187, ALA189, SER190, LEU192, PHE196, GLU276, GLY277, PHE280
Icariside II	-8.77	4	GLU276	SER187, ALA189, LEU192, ASN193, PHE196, LYS197, GLU200, GLY277, PHE280, ILE281

^a Estimated the binding free energy of the ligand receptor complex. ^{b, c} All amino acid residues located 3.13 Å from the original enzyme/compound complex in the AutoDock 4.2 program. ^d Compound 23 (3-({5-[(N-acetyl-3-{4-[(carboxycarbonyl)(2-carboxyphenyl)amino]-1-naphthyl}-L-alanyl)amino]pentyl}oxy)-2-naphthoic acid) and compound 2 (3-(3,5-dibromo-4-hydroxy-benzoyl)-2-ethyl-benzofuran-6-sulfonic acid (4-sulfamoyl-phenyl)-amide) were used as positive ligand.

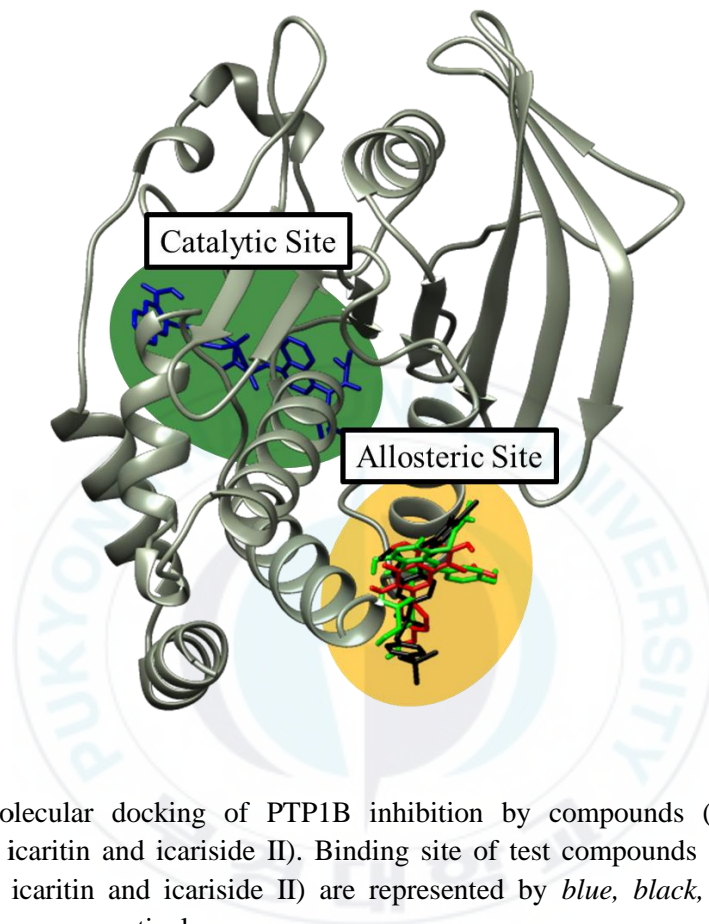


Figure 9. Molecular docking of PTP1B inhibition by compounds (compound 23, compound 2, icaritin and icariside II). Binding site of test compounds (compound 23, compound 2, icaritin and icariside II) are represented by *blue*, *black*, *red* and *green* colored structures, respectively.

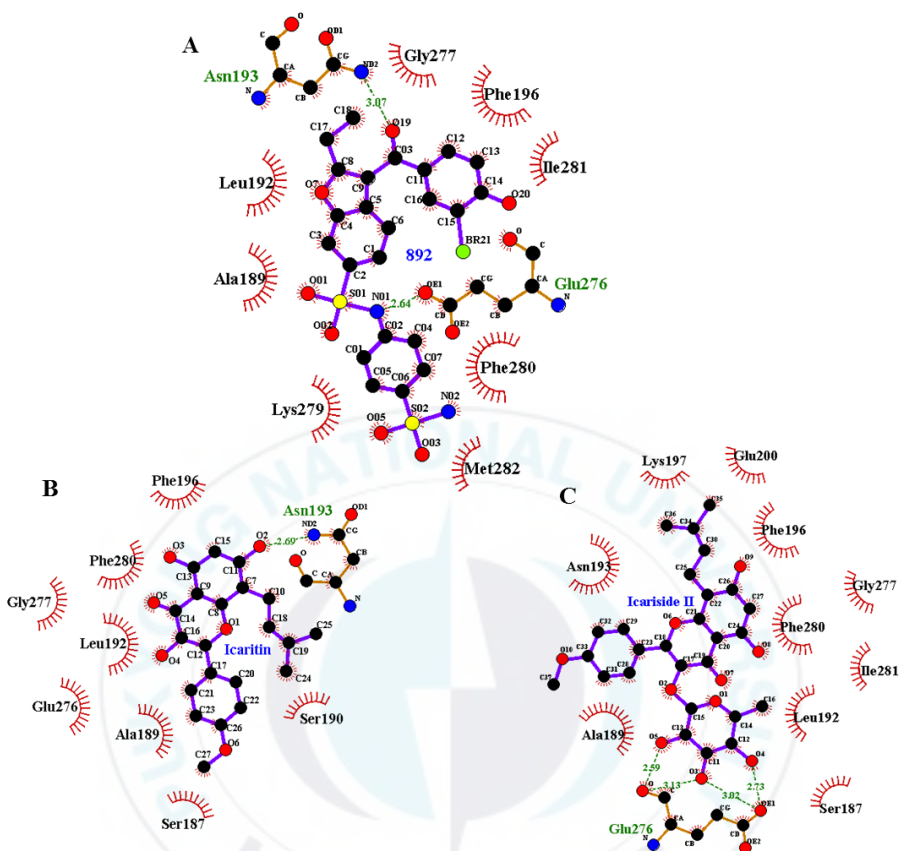


Figure 10. Molecular docking models for PTP1B inhibition of compound 2 (A), icaritin (B) and icariside II (C).

2. Anti-Alzheimer's disease activity

2-1. BACE1 and ChEs inhibitory activities of the MeOH extract and its fractions from aerial parts of *E. koreanum*

In order to investigate the anti-AD potential of the MeOH extract and its fractions from aerial parts of *E. koreanum*, the BACE1, AChE and BChE inhibitory activities were evaluated. The BACE1 inhibitory results of the MeOH extract and its fractions from aerial parts of *E. koreanum* are displayed in Table 5. The CH₂Cl₂ fraction showed potent inhibitory activity against BACE1 dose dependently with IC₅₀ value of 23.82 ± 0.11 µg/mL compared to quercetin used as positive control with IC₅₀ value of 10.27 ± 0.20 µg/mL. In addition, H₂O fraction exhibited moderate BACE1 inhibitory activity with IC₅₀ value of 150.19 ± 0.66 µg/mL. However, MeOH extract, EtOAc and *n*-BuOH fractions showed no BACE1 inhibitory effects under the tested concentrations.

As shown in Figure 11, the MeOH extract of aerial parts of *E. koreanum* showed moderate inhibition against AChE in a dose dependent manner with IC₅₀ value of 53.52 ± 0.33 µg/mL compared to berberine used as positive control with IC₅₀ value of 0.39 ± 0.00 µg/mL. Similarly, the four solvent soluble fractions of the MeOH extract exhibited moderate AChE inhibitory activities in the following order: CH₂Cl₂ fraction (IC₅₀ = 55.59 ± 0.20 µg/mL); EtOAc fraction (IC₅₀ = 65.79 ± 0.36 µg/mL); *n*-BuOH fraction (IC₅₀ = 72.47 ± 1.20 µg/mL); and H₂O fraction (IC₅₀ = 95.70 ± 1.41 µg/mL). Considering yield of fractions and anti-AChE activity, *n*-BuOH fraction is considered the most active fraction.

The BChE inhibitory activity of the MeOH extract from aerial parts of *E. koreanum* exhibited normal inhibitory activity against BChE in a dose dependent manner with IC₅₀

value of $121.33 \pm 2.10 \mu\text{g/mL}$ (Figure 11) compared to berberine used as positive control with IC_{50} value of $7.55 \pm 0.12 \mu\text{g/mL}$. Among the fractions, CH_2Cl_2 fraction showed the highest BChE inhibitory activity with respective IC_{50} value of $92.19 \pm 0.52 \mu\text{g/mL}$. Furthermore, EtOAc, *n*-BuOH and H_2O fractions exhibited moderate BChE inhibitory activities with IC_{50} values of 144.34 ± 6.20 , 294.56 ± 0.23 , and $366.13 \pm 5.96 \mu\text{g/mL}$, respectively. In addition, the selectivity index (SI) is indicated as the ratio IC_{50} value (BChE)/ IC_{50} value (AChE), and the high SI value expresses high AChE selectivity.



Table 5. Inhibitory activities of the MeOH extract and its fractions from *Epimedium koreanum* on BACE1 and ChEs

Samples	Yields (g)	IC ₅₀ (µg/mL) ^a			SI ^b
		BACE1	AChE	BChE	
MeOH extract	665.2	> 300	53.52 ± 0.33	121.33 ± 2.10	2.27
CH ₂ Cl ₂ fraction	56.94	23.82 ± 0.11	55.59 ± 0.20	92.19 ± 0.52	1.66
EtOAc fraction	78.20	> 300	65.79 ± 0.36	144.34 ± 6.20	2.19
<i>n</i> -BuOH fraction	237.12	> 300	72.47 ± 1.20	294.56 ± 0.23	4.06
H ₂ O fraction	268.06	150.19 ± 0.66	95.70 ± 1.41	> 300	3.83
Quercetin ^c	-	10.27 ± 0.20			
Berberine ^c	-		0.39 ± 0.00	7.55 ± 0.12	19.36

^a The 50% inhibitory concentration (IC₅₀) values (µg/mL) were calculated from a log dose inhibition curve and expressed as mean ± S.E.M of triplicate experiments. ^b SI is the AChE selectivity index defined as IC₅₀ BChE/ IC₅₀ AChE affinity ratio. ^c Used as positive control.

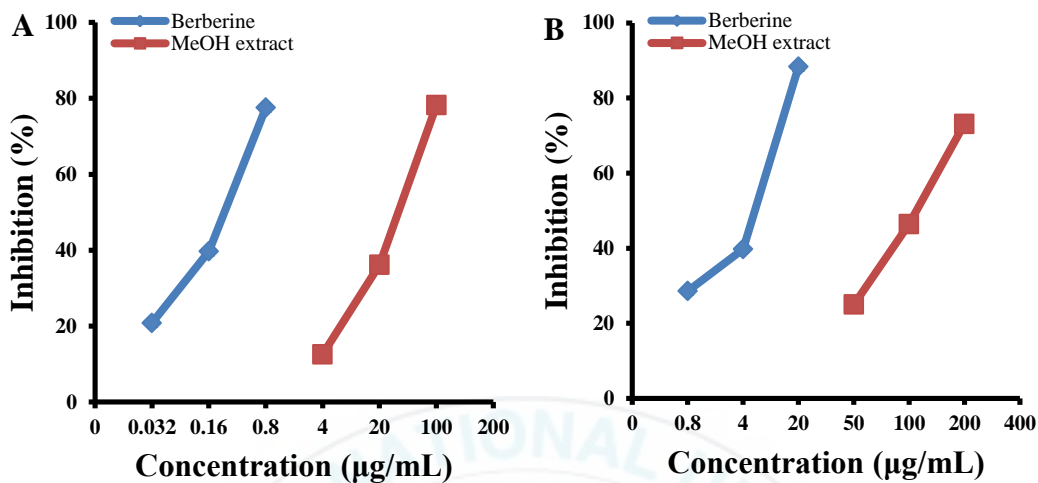


Figure 11. Inhibitory activities of the MeOH extract from *Epimedium koreanum* on AChE (A), BChE (B). All values are expressed as mean \pm S.E.M of triplicate experiments. Berberine was used as positive control.

2-2. BACE1 and ChEs inhibitory activities of the compounds

The BACE1 inhibition was seen with IC_{50} of $35.90 \pm 5.12 \mu\text{M}$ for icaritin, $38.34 \pm 2.65 \mu\text{M}$ for icariside II and $79.02 \pm 5.12 \mu\text{M}$ for icariin compared to the positive control quercetin ($IC_{50} = 34.01 \pm 0.65 \mu\text{M}$). While epimedin A and epimedin B showed moderate inhibitory activities with IC_{50} values of 130.22 ± 3.94 and $154.19 \pm 7.50 \mu\text{M}$, respectively. However epimedin C exhibited no BACE1 inhibitory effects at the concentration up to $300 \mu\text{M}$.

As shown in Table 6, icariin, icaritin, epimedin A, epimedin B and epimedin C exhibited the most potent inhibitory activities against AChE with IC_{50} values of 26.50 ± 0.97 , 30.13 ± 0.34 , 26.65 ± 0.36 , 31.74 ± 0.28 and $30.88 \pm 0.71 \mu\text{M}$, accordingly, compared with berberine ($IC_{50} = 0.81 \pm 0.05 \mu\text{M}$). The AChE inhibitory activity suggested that the icariin having α -L-rhamnose and β -D-glucose moiety linked through the C-3 and C-7 of prenylated flavonol exhibited potent activity. In addition, epimedin A, epimedin B and epimedin C, which have the β -D-glucose, β -D-xylose and α -L-rhamnose moiety linked through α -L-rhamnose of icariin, showed similar activity compared to icariin. While icariside II having only α -L-rhamnose moiety at C-3 of flavonol showed low AChE inhibitory activity with IC_{50} value of $75.88 \pm 0.88 \mu\text{M}$. However, the rest of the compounds magnolol and (-)-syringaresinol showed no AChE inhibitory activity at the concentration up to $300 \mu\text{M}$.

Among the tested compounds, icariin, epimedin A and epimedin C showed moderate effect against BChE with IC_{50} values of 269.43 ± 1.95 , 210.80 ± 2.36 and $208.74 \pm 0.06 \mu\text{M}$, respectively, compared with berberine ($IC_{50} = 26.35 \pm 0.07 \mu\text{M}$). However icaritin, icariside II, epimedin B, magnolol and (-)-syringaresinol exhibited no BChE inhibitory activity under the tested concentrations. The SI values of active compounds were obtained in a range of 6.76 to 10.17 (Table 6).

Table 6. Inhibitory activities of compounds of *Epimedium koreanum* on BACE1 and ChEs

Compounds	IC ₅₀ (μM) ^a			SI ^b
	BACE1	AChE	BChE	
Icariin	79.02 ± 5.13	26.50 ± 0.97	269.43 ± 1.95	10.17
Icaritin	35.90 ± 5.12	30.13 ± 0.34	> 300	-
Icariside II	38.34 ± 2.65	75.88 ± 0.88	> 300	-
Epimedin A	130.22 ± 3.94	26.65 ± 0.36	210.80 ± 2.36	7.91
Epimedin B	154.19 ± 7.50	31.74 ± 0.28	> 300	-
Epimedin C	> 300	30.88 ± 0.71	208.74 ± 0.06	6.76
Magnolol	NA ^d	> 300	> 300	-
(-)-Syringaresinol	NA ^d	> 300	> 300	-
Quercetin ^c	34.01 ± 0.65			
Berberine ^c		0.81 ± 0.05	26.35 ± 0.07	32.53

^a The 50% inhibitory concentration (IC₅₀) values (μM) were calculated from a log dose inhibition curve and expressed as mean ± S.E.M of triplicate experiments. ^b SI is the AChE selectivity index defined as IC₅₀ BChE/IC₅₀ AChE affinity ratio. ^c Used as positive control. ^d Not analyzed.

2-3. Molecular docking simulation in BACE1 inhibition

Molecular docking simulation study was performed to validate the mechanism of the interaction between compounds and the active site of BACE1. In this study, the 3D docking of active compounds (icaritin and icariside II) were simulated, where 2-amino-3-{{(1R)-1-cyclohexyl-2-[(cyclohexylcarbonyl)amino]ethyl}- 6-phenoxyquinazolin-3-ium (positive ligand of catalytic model of BACE1, QUD) and 5,7,4'-trimethoxyflavone (positive ligand of allosteric model, TMF) were considered as the standard ligand to compare the orientation of the tested compounds. The docking analysis were conducted to validate structure-activity relationship of compounds with the obtained experimental data as well as used to evaluate the binding site-directed inhibition of BACE1. The AutoDock 4.2 program uses a semi-empirical free energy force field to guess the binding complexes of protein-ligand of a known structure and the binding energies for bound state. The results of docking simulations of compounds are shown in Table 7 and Figure 12. The BACE1-icaritin complex showed -7.8 kcal/mol of binding energy with four hydrogen bonds interacting with TYR198, ASP228, GLY230 and THR231. The oxygen group of TYR198 was involved in the strong hydrogen bonding with the hydroxyl group (O3) of icaritin with bond distance of 2.96 \AA . In addition, the hydroxyl group (O4) of icaritin was associated with the hydrogen bonding interaction with the oxygen groups of ASP228, GLY230 and THR231 having 3.10 , 2.93 and 2.92 bond distances, respectively (Figure 13). Moreover, hydrophobic interactions were also exhibited between GLN12, LEU30, ASP32, TYR71 and PHE108. These hydrophobic interactions are important to intensify the protein-ligand interaction and for positioning of icaritin in the active pocket to inhibit BACE1 activity. The result of molecular docking simulation of icariside II in BACE1 showed that icariside II was located in both of the catalytic and allosteric site of BACE1. The binding energy of catalytic BACE1-icariside II complex was -8.1 kcal/mol with four hydrogen bonds interacting with ASP32, LYS224, THR231 and THR329. The

oxygen groups of ASP32 and THR231 were involved in the hydrogen bonding interaction with the hydroxyl groups (O5 and O8) of icariside II with bond distances 2.92 and 2.66 Å, respectively (Figure 13). In addition, the hydroxyl group (O9) of icariside II was associated with hydrogen bonding interactions with oxygen group of THR329 and nitrogen group of LYS224 having respective 3.06 and 2.80 bond distances Å (Figure 13). The hydrophobic interactions were also observed between GLY34, SER35, ASN37, VAL69, TYR71, PHE108, ILE118, ARG128, TYR198, ASP228 and VAL332. These hydrophobic interactions provide further stability to the complex and help to fit thoroughly in the active pocket of BACE1. In contrast, binding energy of allosteric BACE1-icariside II complex was -7.6 kcal/mol with three hydrogen bonds interacting with VAL309, GLU310 and GLU339. The oxygen groups of VAL309 and GLU310 were associated with hydrogen bonding interaction with hydroxyl group (O4) of icariside II having 2.96 and 3.12 Å bond distances, individually. Moreover, the hydrophobic interactions were also observed between SER10, GLY156, ALA157, ALA168, VAL170, TRP277, GLN303, LEU306, PRO308, TYR320 and VAL361. Therefore, the hydrogen and hydrophobic interactions with BACE1 might be associated with the hydrolysis of substrate molecule. The molecular docking simulation result was corresponded well with the experimental data with respect to the BACE1 inhibitory activity of compounds.

Table 7. Binding site residues and docking scores of compounds in β -site APP cleaving enzyme 1 (BACE1) using AutoDock 4.2 program

Compounds	Binding energy ^a (kcal/mol)	No. of H-bond	H-bond interacting residues ^b	Van der Waals bond interacting residues ^c
QUD ^d (catalytic inhibitor)	-8.48	4	ASP32, ASP228, GLY230	LEU30, GLY34, SER35, TYR71, GLN73, GLY74, LYS75, ASP106, LYS107, PHE108, ILE118, TYR198, ILE226, THR231, ASG235, VAL332
TMF ^d (allosteric inhibitor)	-6.43	0	-	SER10, GLY11, ARG30, GLY156, ALA157, THR232, GLN303, GLN304, PRO308, ALA323, VAL336, GLU339, VAL361
Icaritin	-7.8	4	TYR198, ASP228, GLY230, THR231	GLN12, LEU30, ASP32, TYR71, PHE108
Icariside II	-8.1	4	ASP32, LYS224, THR231, THR329	GLY34, SER35, ASN37, VAL69, TYR71, PHE108, ILE118, ARG128, TYR198, ASP228, VAL332
	-7.6	3	VAL309, GLU310, GLU339	SER10, GLY156, ALA157, ALA168, VAL170, TRP277, GLN303, LEU306, PRO308, TYR320, VAL361

^a Estimated the binding free energy of the ligand receptor complex. ^{b, c} All amino acid residues located 3.33 Å from the original enzyme/compound complex in the AutoDock 4.2 program. ^d QUD (2-amino-3-((1R)-1-cyclohexyl-2-[(cyclohexylcarbonyl)amino]ethyl)-6-phenoxyquinazolin-3-ium) and TMF (5,7,4'-trimethoxyflavone) were used as positive ligand.

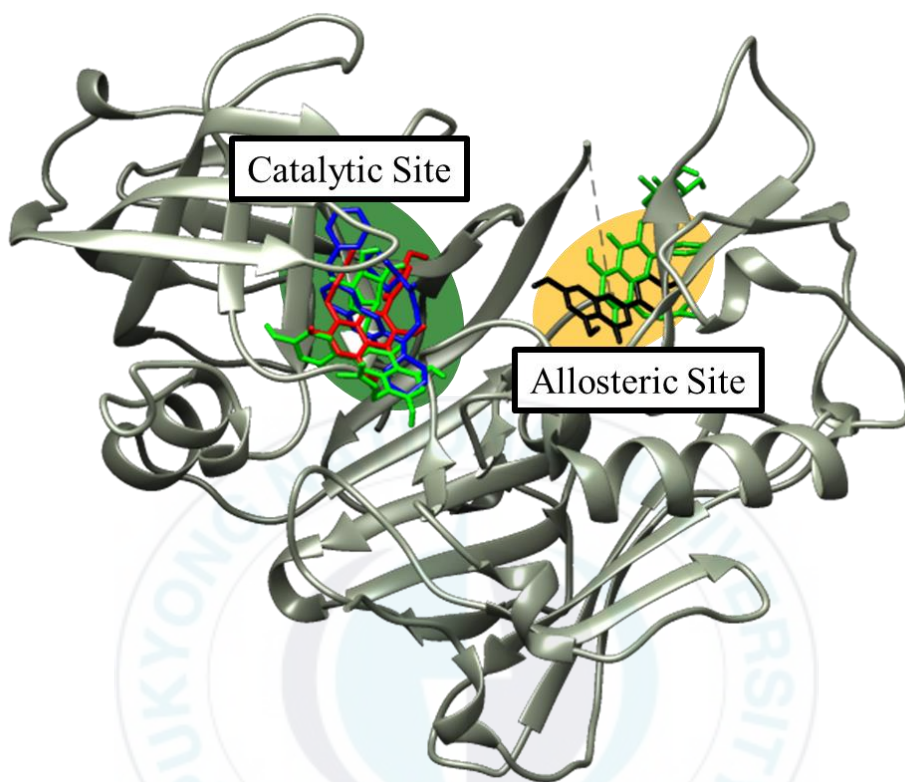


Figure 12. Molecular docking of BACE1 inhibition by compounds (QUD, TMF, icaritin and icariside II). Binding sites of test compounds (QUD, TMF, icaritin and icariside II) are represented by *blue, black, red* and *green* colored structures, respectively.

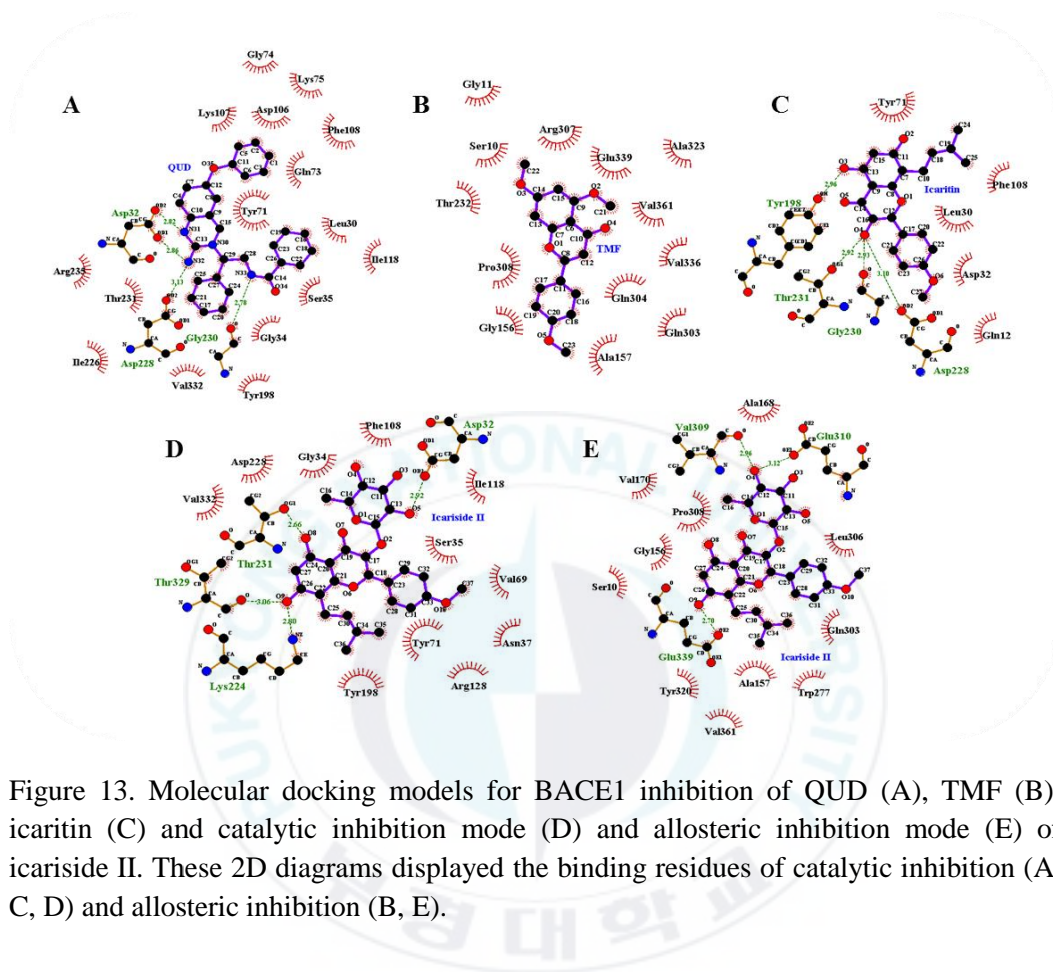


Figure 13. Molecular docking models for BACE1 inhibition of QUD (A), TMF (B), icaritin (C) and catalytic inhibition mode (D) and allosteric inhibition mode (E) of icariside II. These 2D diagrams displayed the binding residues of catalytic inhibition (A, C, D) and allosteric inhibition (B, E).

2-4. Enzyme kinetic analysis of compounds with AChE

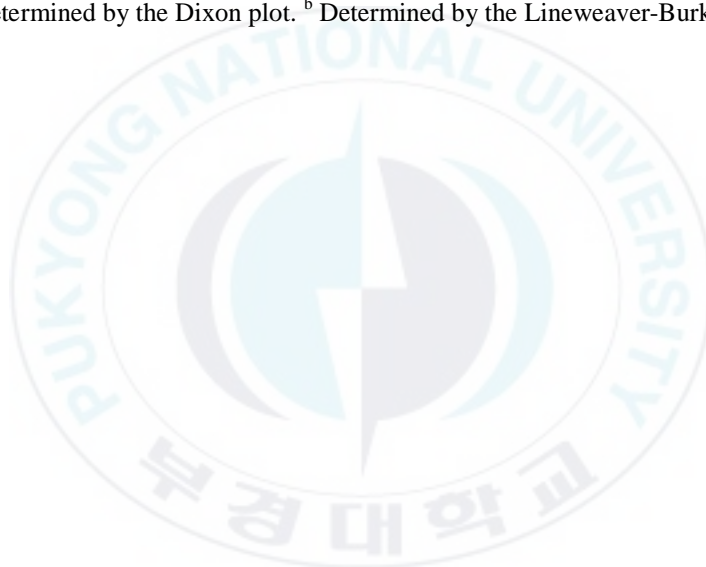
The result from AChE inhibitory activity demonstrated that among the tested compounds, five were found to be active (icariin, icaritin, epimedin A, epimedin B and epimedin C). Therefore, these compounds were further analyzed to demonstrate the correlation of compounds with substrate (ATCh) in AChE. All of the tested compounds showed noncompetitive-type inhibition against AChE (Figure 14 and 15). In addition, the K_i values of icariin, icaritin, epimedin A, epimedin B and epimedin C were 26.32, 32.46, 20.32, 27.75 and 25.55 μM , respectively.



Table 8. Enzyme kinetic analysis of compounds of *E. koreanum* with AChE

Test compounds	K_i (μM) ^a	Inhibition type ^b
Icariin	26.32	Non-competitive
Icaritin	32.46	Non-competitive
Epimedin A	20.32	Non-competitive
Epimedin B	27.75	Non-competitive
Epimedin C	25.55	Non-competitive

^a Determined by the Dixon plot. ^b Determined by the Lineweaver-Burk plot.



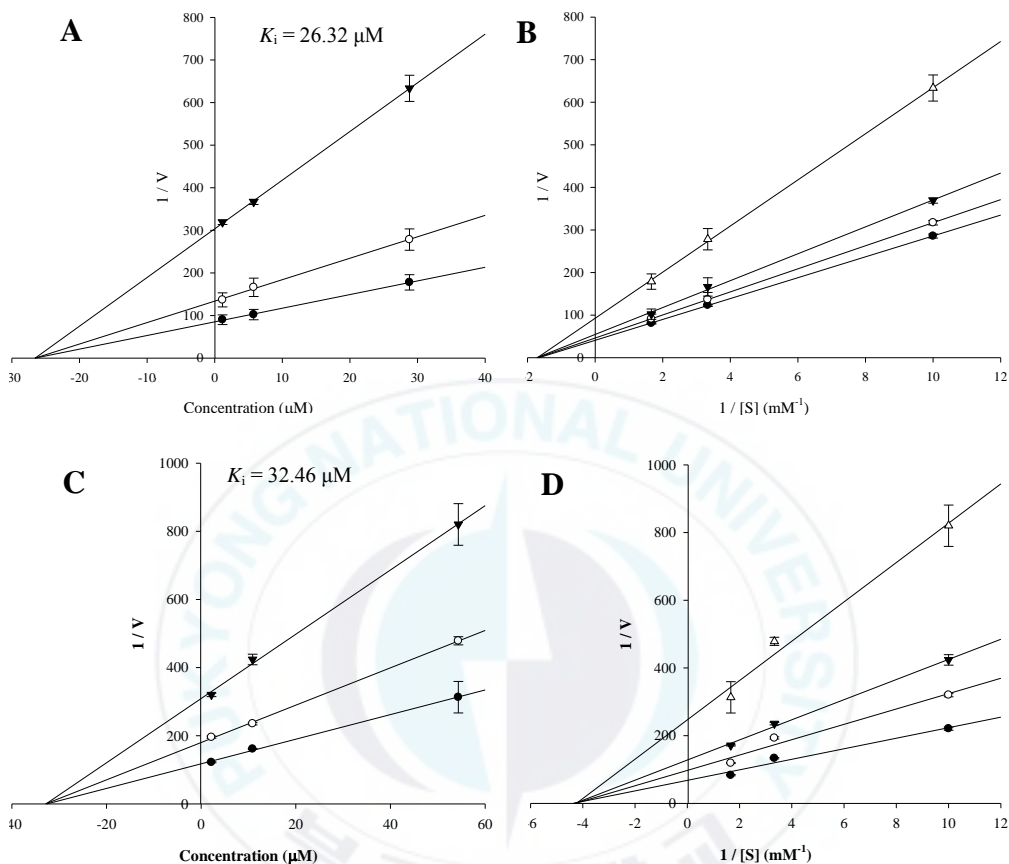


Figure 14. Dixon and Lineweaver-Burk plots of the inhibition of AChE by icariin and icaritin. The results showed the effects of the presence of different concentrations of the substrate (0.6 mM (●), 0.3 mM (○) and 0.1 mM (▼) for (A) icariin and (C) icaritin and the effect of the presence of different concentration of (B) icariin (0 μM (●), 1.15 μM (○), 5.76 μM (▼) and 28.82 μM (Δ)) and (D) icaritin (0 μM (●), 2.17 μM (○), 10.87 μM (▼) and 54.35 μM (Δ)).

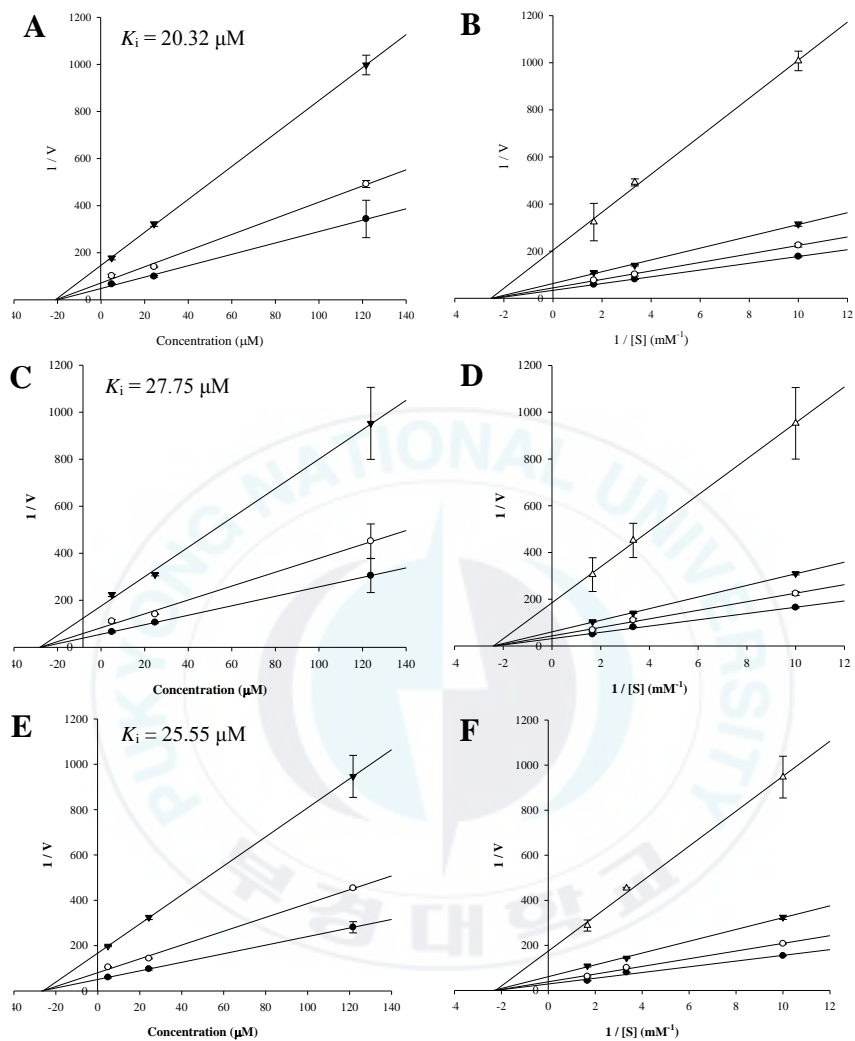


Figure 15. Dixon and Lineweaver-Burk plots of the inhibition of AChE by epimedins A, epimedins B and epimedins C. The results showed the effects of the presence of different concentrations of the substrate (0.6 mM (●), 0.3 mM (○) and 0.1 mM (▼)) for (A) epimedins A, (C) epimedins B and (E) epimedins C and the effect of the presence of different concentration of (B) epimedins A (0 μM (●), 4.87 μM (○), 24.33 μM (▼) and 121.65 μM (Δ)), (D) epimedins B (0 μM (●), 4.95 μM (○), 24.75 μM (▼) and 123.76 μM (Δ)) and (F) epimedins C (0 μM (●), 4.87 μM (○), 24.33 μM (▼) and 121.65 μM (Δ)).

2-5. Molecular docking simulation in AChE inhibition

For the determination of the exact orientation of compounds in the active site of AChE, icariin, icaritin, epimedin A, epimedin B and epimedin C were simulated and compared with the reported ligand, tacrine and E2020 by AutoDock 4.2 results. The results of docking simulation of compounds are shown in Table 9 and Figure 16. The AChE-icariin complex showed -9.51 kcal/mol of binding energy with four hydrogen bonds interacting with PHE288 and ARG289. The nitrogen groups of PHE288 and ARG289 were associated with the hydrogen bonding interactions with the hydroxyl group (O4 and O5) of icariin having 2.99 and 2.69 Å bond distance, respectively, and oxygen group of ARG289 was involved in hydrogen bond interactions with the hydroxyl groups (O4 and O5). Some hydrophobic interactions were involved with GLN69, TYR70, ASP72, GLN74, TRP84, ASN85, PRO86, GLY118, TYR121, SER122, TRP279, LEU282, ILE287, PHE290, PHE330, PHE331, TYR334 and HIS440 interacting residues. The binding energy of AChE-icaritin complex was -8.12 kcal/mol with one hydrogen bonds interacting with PHE288. The nitrogen group of PHE288 was involved in the hydrogen bonding interaction with O6 of icaritin with bond distance of 3.03 Å. Moreover, hydrophobic interactions were also observed between TYR70, ASP72, TRP84, TYR121, TRP279, ILE287, PHE290, PHE330, PHE331 and TYR334. On the other hand, the AChE-epimedin A, -epimedin B and -epimedin C complexes showed -6.51 , -6.25 and -7.66 kcal/mol of binding energy with two, four and six hydrogen bond interactions, respectively. In the AChE-epimedin A complex, the oxygen group of TYR121 was involved in the hydrogen bonding interaction with O15 of epimedin A with bond distance of 3.04 Å, and the oxygen group of TYR70 was associated with the hydrogen bonding interaction with O12 of epimedin A having 2.70 Å bond distance. The hydrophobic interactions were exhibited between ASP72, GLN74, GLY118, TRP279, LEU282, SER286, ILE287, PHE288, PHE290, PHE330, PHE331, TYR334 and HIS440.

In addition, the oxygen group of TYR70 and ASN85 were associated with the hydrogen bonding interaction with O12 and O5 of epimedin B having 2.91 and 2.48 Å bond distances, correspondingly, and the oxygen group of SER122 was involved in the hydrogen bonding interactions with O6 and O11 of epimedin B with bond distances of 2.58 and 2.65 Å. The hydrophobic interactions were exhibited between ASP72, SER81, TRP84, GLY117, GLY118, GLY119, TYR121, SER200, TRP279, SER286, ILE287, PHE288, ARG289, PHE290, PHE331 and TYR334. Meanwhile, the oxygen group of TYR70 was involved in the hydrogen bonding interaction with O12 of epimedin C with bond distances of 2.87 Å, and the oxygen group of ASN85 was associated with the hydrogen bonding interaction with O5 of epimedin C having 2.42 Å bond distance. In addition, the oxygen group of SER122 was involved in the hydrogen bonding interactions with O6 and O11 of epimedin C with bond distances of 2.47 and 3.17 Å. Furthermore, the oxygen group of SER286 was associated with the hydrogen bonding interactions with O15 and O17 of epimedin C having 2.58 and 2.93 Å bond distances. Moreover, the hydrophobic interactions were observed between ASP72, SER81, TRP84, GLY117, GLY118, GLY119, TYR121, SER200, TRP279, ILE287, PHE288, ARG289, PHE290, LEU282, PHE330, PHE331, TYR334 and HIS440.

Table 9. Binding site residues and docking scores of compounds in acetylcholinesterase (AChE) using AutoDock 4.2 program

Compounds	Binding energy ^a (kcal/mol)	No. of H-bond	H-bond interacting residues ^c	Van der Waals bond interacting residues ^d
Tacrine ^e (catalytic inhibitor)	-9.5	1	HIS440	ASP72, GLY80, SER81, TRP84, GLU199, PHE330, TYR334, TRP432, ILE439, GLY441, TYR442
E2020 ^e (allosteric inhibitor)	-11.06	0	-	GLN69, TYR70, ASP72, SER81, TRP84, ASN85, TYR121, SER122, TRP279, ILE287, ARG289, PHE290, PHE330, PHE331, TYR334, GLY335
Icariin	-9.51	4	PHE288, ARG289	GLN69, TYR70, ASP72, GLN74, TRP84, ASN85, PRO86, GLY118, TYR121, SER122, TRP279, LEU282, ILE287, PHE290, PHE330, PHE331, TYR334, HIS440
Icaritin	-8.12	1	PHE288	TYR70, ASP72, TRP84, TYR121, TRP279, ILE287, PHE290, PHE330, PHE331, TYR334
Epimedin A	-6.51	2	TYR70, TYR121	ASP72, GLN74, GLY118, TRP279, LEU282, SER286, ILE287, PHE288, PHE290, PHE330, PHE331, TYR334, HIS440
Epimedin B	-6.25	4	TYR70, ASN85, SER122	ASP72, SER81, TRP84, GLY117, GLY118, GLY119, TYR121, SER200, TRP279, SER286, ILE287, PHE288, ARG289, PHE290, PHE331, TYR334
Epimedin C	-7.66	6	TYR70, ASN85, SER122, SER286	ASP72, SER81, TRP84, GLY117, GLY118, GLY119, TYR121, SER200, TRP279, ILE287, PHE288, ARG289, PHE290, LEU282, PHE330, PHE331, TYR334, HIS440

^a Estimated the binding free energy of the ligand receptor complex. ^b A number of hydrogen bond between compounds and active site of AChE. ^{c, d} All amino acid residues located 3.33 Å from the original enzyme/compound complex in the AutoDock 4.2 program. ^e Tacrine and E2020 (1-benzyl-4[(5,6-dimethoxy-1-indanon-2-yl)methyl]piperidine) were used as positive ligand.

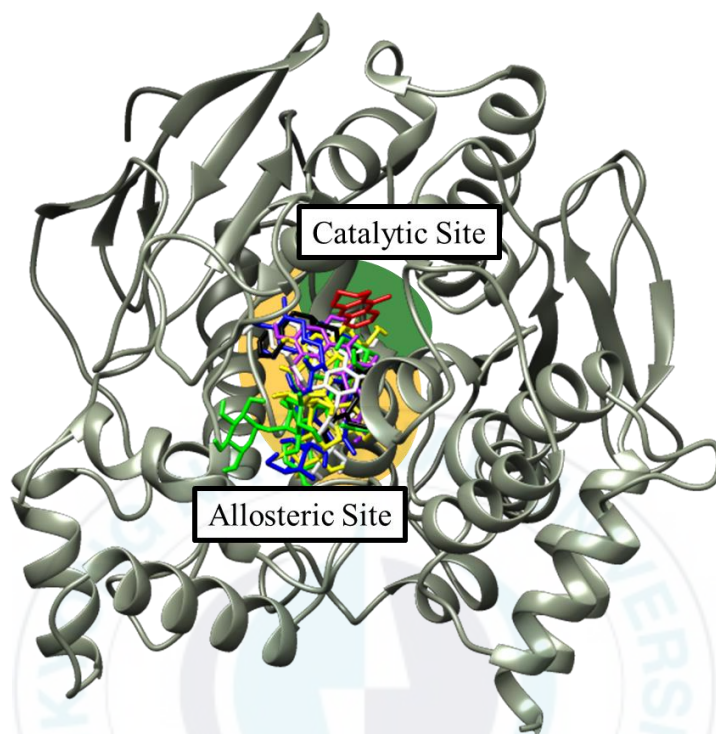


Figure 16. Molecular docking of AChE inhibition by compounds (Tacrine, E2020, icariin, icaritin, epimedine A, epimedine B and epimedine C). Binding sites of test compounds (Tacrine, E2020, icariin, icaritin, epimedine A, epimedine B and epimedine C) are represented by red, black, white, purple, green, blue and yellow colored structures, respectively.

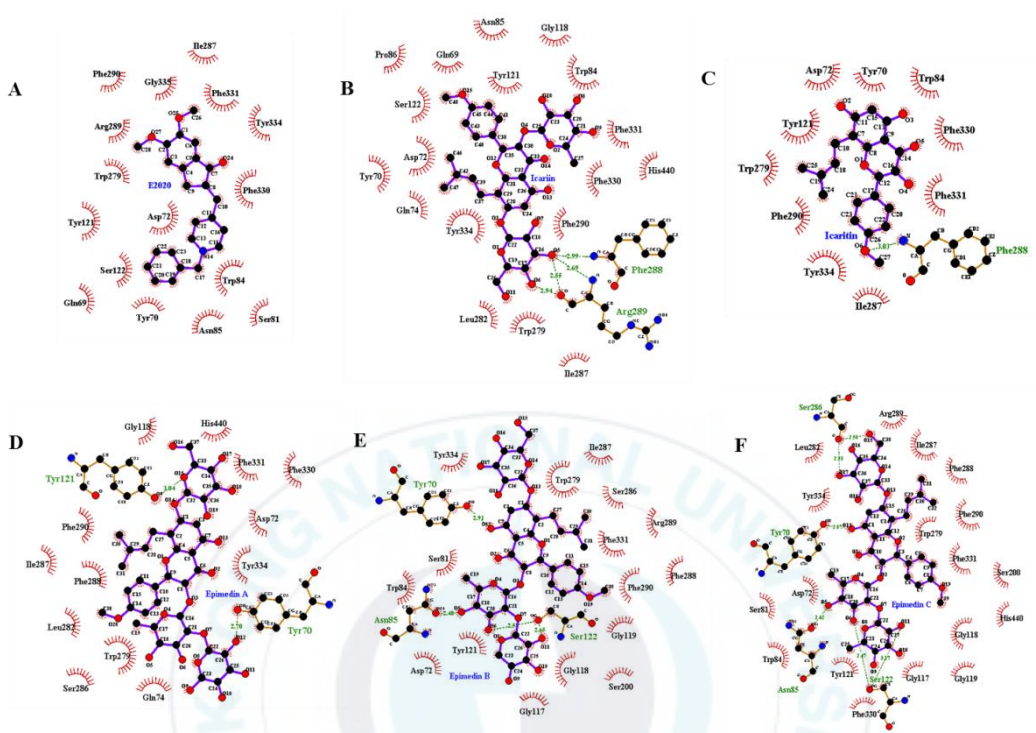


Figure 17. Molecular docking models for AChE inhibition of E2020 (A), icaritin (B), icaritin (C), epimedin A (D), epimedin B (E) and epimedin C (F).

IV. Discussion

DM is a major community concern and epidemiological studies revealed it's ever increasing prevalence which almost attained epidemic proportions worldwide. As of 2015, more than 415 million adults have DM, and this number is expected to rise up to 642 million by 2040 (IDF, 2015). Over the past decade, the growing epidemic of DM and its associated complications has offered both challenges and opportunities. Massive developments have been seen which presented several therapeutic approaches and many novel chemical entities have been introduced to treat diabetes; however, long-term safety, efficacy of these chemicals are still leaving several concerns. Thus, finding new natural drug candidates for DM, with no side effects are important for the treatment and prevention to diabetes. PTP1B acts as a negative regulator of the insulin metabolic pathway, and α -glucosidase promotes the absorption of carbohydrates into blood vessel by hydrolyzing oligosaccharide to glucose. Therefore, new inhibitors of PTP1B and α -glucosidase are needed to develop the drugs for diabetes. *E. koreanum* is used as TCM to treat impotence, infertility in woman, dysuria, rheumatic arthritis, geriatric depression, angina pectoris (Nakashima et al., 2016; Chen et al., 2015). In this study, despite the wide pharmacological effects of *E. koreanum*, there has been no systematic investigation which offers the possibility of developing anti-DM drug candidates from *E. koreanum*.

AD, the most common cause of dementia in the elderly, is a progressive neurodegenerative disease. The dementia is clinically characterized by progressive cognitive decline, psycho-behavior disturbances, and memory loss (Herrmann et al., 2011). The worldwide prevalence of dementia in 2006 was over 25 million, and

epidemiologists predict this number to reach over 80 million by 2040, highlighting increased concerns about the future social and economic burden (Ferri et al., 2006). Therefore, the natural drugs are necessary in order to treat AD patients. A β plays an important role in the pathogenesis of AD, and was formed *via* the cleavage of APP by β - or γ -secretases (Butterfield et al., 2007). The accumulation of A β has been implicated with critical memory loss and neuronal cell death (Selkoe, 2002). Thus, BACE1 inhibition has been emerged as promising therapeutic targets for treatment of AD. The agents for AD treatment such as rivastigmine, donepezil and tacrine were clinically used and developed, and these agents showed enhancement in the cognitive function of AD patients. However, some agents induce side effects including diarrhea, dizziness, hepatotoxicity and gastroenteric trouble (Bond et al., 2012). Therefore, natural products need to be developed for the prevention of AD. In addition, the treatment for AD has mostly involved in the metabolism of neurotransmitters that are known to be lacking in AD. A loss in central cholinergic transmission caused by degeneration of the basal forebrain nuclei is a vital pathological and neurochemical characteristic of AD (Bartus et al., 1982). Pharmacological treatment of AD is based on using inhibitors of ChEs, which have positive properties on cognitive, functional, and behavioral symptoms of the disease, but their role in AD pathogenesis is unclear (Schelterns and Feldman, 2003). AChE and BChE both are regarded as the crucial enzyme in cholinergic transmission which hydrolyzes the ester bond of ACh in cholinergic synapses (Mesulam et al., 2002). In the normal brain, AChE indicated almost 80% of ChE activity (Greig et al., 2001). Thus, AChE inhibitors may offer high ability for treatment of AD patients. Furthermore, M de la Monte, S (2012) demonstrated that in the initial stages of AD, it accompanied with impairments in cerebral glucose utilization. In recent years, emerging data suggested that deficits in glucose, impaired insulin signaling and brain insulin resistance are common in the pathogenesis of AD; thus, some studies even called AD type 3 DM (Chen et al., 2014; Feng et al., 2016).

As summarized in Table 1, the anti-DM activity of the MeOH extract was attempted, along with the CH₂Cl₂, EtOAc, *n*-BuOH, and H₂O fractions using the *in vitro* PTP1B and α -glucosidase assays. Based on obtained results, the MeOH extract of aerial parts of *E. koreanum* exhibited PTP1B and α -glucosidase inhibitory effects dose-dependently (Figure 7). Among the four solvent soluble fractions, the CH₂Cl₂ fraction showed potent both of PTP1B and α -glucosidase inhibitory activity compared to the other fractions. In addition, icaritin and icariside II showed inhibitory potential with IC₅₀ value of 11.94 \pm 0.15 and 9.94 \pm 0.15 μ M against PTP1B, and 74.42 \pm 0.01 and 106.59 \pm 0.44 μ M against α -glucosidase. In conclusion, icaritin and icariside II, which are deglycosylated metabolites of icariin, may play important roles on PTP1B and α -glucosidase enzyme inhibition. In previous study, *E. koreanum* extract has been pharmacologically and biologically evaluated such as osteoblastic proliferation stimulating activity (Meng et al., 2005), intervention effects on kidney-yang deficiency syndrome (Huang et al., 2013) and estrogenic activity (Islam et al., 2012). In addition, Oh et al. (2013) reported that the EH extract has significant anti-diabetic activity in streptozotocin induced diabetic rats. Moreover, Icaritin and icariside II from *E. koreanum* also showed potent anti-diabetic activities, and the potencies of these compounds were first time reported in this study. Furthermore, epimedin A-C were inactive on α -glucosidase inhibitory activity similar with the reported study (Phan et al., 2013).

To establish their mode of inhibition, the enzyme kinetics and the molecular docking studies were performed with compounds displayed high inhibitory activities (icaritin and icariside II). Lineweaver-Burk and Dixon plots for the kinetic study demonstrated that both of active compounds exhibited non-competitive inhibition against PTP1B to decrease the V_{max} values without changing the K_m values with K_i value of 11.41 and 11.66 μ M (Table 3 and Figure 8). In order to predict binding sites and affinities, the molecular docking simulation was performed. The best docked conformation was selected based on

binding affinity, hydrogen bonding and hydrophobic interactions. In addition, the amino acid residues of enzyme are associated with both H-bond and hydrophobic interactions with compounds (Kumar et al., 2014). Computational docking simulation provides thorough and vital information to understand the mechanism behind active site binding interactions (Seong et al., 2016). In order to avoid the bottleneck in the PTP1B inhibitor development, allosteric PTP1B inhibitors have been focused. Allosteric sites have higher specificity, fewer side effects and lower toxicity (Baskaran et al., 2012; Huang et al., 2014). The allosteric site is located on the C-terminal domain of PTP1B and is bordered on helices $\alpha 3$, $\alpha 6$ and $\alpha 7$, which constitute a hydrophobic pocket for allosteric inhibitors (Li et al., 2014). The WPD loop, which contributes to the recognition of acid/base ASP181, is the primary determinant for the binding of catalytic substrate in PTP1B, and the allosteric inhibition effect on PTP1B was associated with the closure of the catalytic WPD loop (Lee and Wang, 2007; Choi et al., 2015). In the presence of allosteric inhibitors, the WPD loop changes conformation compared to the Apo form of PTP1B (Murray, 2005; Li et al., 2014). Compound 2, which is a positive inhibitor of allosteric PTP1B model, forms two hydrogen bonds with allosteric sites of PTP1B such as ASP193 and GLU276 (Table 4 and Figure 10A). The hydroxyl group of icaritin was interacted with PTP1B forming single hydrogen bond with ASN193 showing a -6.24 kcal/mol binding energy (Figure 10B). In addition, icariside II showed a lower binding score, indicating high affinity, with PTP1B than icaritin. The GLU276 was interacted with the hydroxyl groups of α -L-rhamnose moiety of icariside II by forming four hydrogen bonds (Figure 10C). The hydrophobic interactions contributed to produce the higher binding affinity between PTP1B and compounds. The result of molecular docking simulation is in accordance with the results of *in vitro* PTP1B inhibitory assay that icariside II and icaritin showed potent inhibitory activity (Table 2).

Recently, Wu et al. (2016) demonstrated that icariin was hydrolyzed to icariside II and

icaritin by human intestinal microflora (Figure 18). In addition, some studies revealed that icariin has an amelioration effect in streptozotocin-induced diabetic retinopathy (Xin et al., 2012), reduces mitochondrial oxidative stress injury in diabetic rat hearts (Bao and Chen, 2011), and protects cisplatin-induced acute renal injury in mice (Ma et al., 2015). Furthermore, icariside II ameliorates diabetic nephropathy in streptozotocin-induced diabetic rats (Tian et al., 2015), and icaritin reported anti-inflammatory and anti-oxidative stress effects in rats (Zhang et al 2015). Depending on this study, reported *in vivo* potential of icariin is attributed to the activity of its metabolites, icariside II or icaritin.

As summarized in Table 5, characterization of the BACE1 and ChEs inhibitory activities of the MeOH extracts was attempted, along with the CH₂Cl₂, EtOAc, *n*-BuOH and H₂O fractions using the *in vitro* BACE1, AChE and BChE assays. Based on results, the MeOH extract of aerial parts of *E. koreanum* exhibited ChEs inhibitory effects in a dose-dependent manner (Figure 11), while it showed no BACE1 inhibitory activity. Among the four solvent soluble fractions, the CH₂Cl₂ fraction showed most potent inhibitory activity against BACE1 and AChE and BChE (IC₅₀ = 23.82 ± 0.11, 55.59 ± 0.20 and 92.19 ± 0.52 µg/mL, respectively) compared to the other fractions. In addition, the compounds were screened for their BACE1 and ChEs inhibitory activities at different concentrations. Tested compounds inhibited each enzyme with IC₅₀ values ranging from 35.90 to 154.19 µM against BACE1, and 26.50 to 75.88 µM against AChE, as well as 208.74 to 269.43 µM against BChE (Table 6). Similarly with PTP1B inhibitory activity, icariside II and icaritin, which are icariin metabolites, showed potent inhibitory activity against BACE1 displayed IC₅₀ values of 35.90 ± 5.12 and 38.34 ± 2.65, respectively. Furthermore, the result of molecular docking simulation suggests that icariside II and icaritin are competitive and mixed-type inhibitors. In order to predict binding sites and affinities the molecular docking simulation was performed. BACE1 consists of two main

domains, which are the N-terminal domain and the C-terminal domain, and numerous detailed sub-regions are distributed between them. The most important regions of the BACE1 recognized as 10s loop and flap assist the entry and binding of a substrate at the active site *via* their movements (Barman and Prabhakar, 2013). The two aspartate residues in the cleft of the active site, ASP32 and ASP228 conserve the catalytic site of BACE1 (Hernández-Rodríguez et al., 2016). These residues have been demonstrated in the catalytic functioning of the entire family of aspartyl proteases. In addition, the presence of TYR71 in the flap regulates the open/closed conformation in BACE1 (Hong et al., 2000). In contrast, the residues of allosteric site of BACE1 are SER10, THR232, VAL336 and ALA157 (Youn et al., 2016). QUD, which is positive inhibitor of catalytic BACE1 model, forms four hydrogen bonds with catalytic site of BACE1 such as ASP32 and ASP228 (Table 7 and Figure 13A). The hydroxyl group of icaritin was interacted with catalytic residue ASP228 of BACE1 forming hydrogen bond (Figure 13C). In addition, icariside II was located in both of catalytic and allosteric site of BACE1. The ASP32 of catalytic site was interacted with the hydroxyl groups of α -L-rhamnose moiety of icariside II by forming hydrogen bond (Figure 13D). Moreover, the residues of allosteric site such as SER10 and ALA157 were interacted with icariside II by forming hydrophobic interactions (Figure 13E). The hydrophobic interactions contributed to produce the higher binding affinity between BACE1 and compounds. The result of molecular docking simulation is in accordance with the results of *in vitro* BACE1 inhibitory assay that icariside II and icaritin showed potent inhibitory activity (Table 6). Although present study didn't perform the kinetic analysis of BACE1, the inhibition mode of active compounds can be suggested according to docking simulation results.

The high SI value proposed that inhibitors have more activity to AChE in human brain. The SI values of active compounds showed ranging from 6.76 to 10.17, and indicated that the icariin, epimedin A and epimedin C are considered as AChE-selective inhibitors.

Among the tested compounds, icariin having α -L-rhamnose and β -D-glucose moiety linked through the C-3 and C-7 of prenylated flavonol exhibited the highest inhibitory activity. In addition, epimedidin A, epimedidin B and epimedidin C showed similar inhibitory activities compared to icariin. Although icaritin has no glucosidic moiety, it exhibited comparable inhibitory activity with icariin. However, icariside II which has only α -L-rhamnose moiety linked through C-3 of prenylated flavonol exhibited moderate inhibitory effect. According to the results, glycosylation at C-3 and C-7 of prenylated flavonol of *E. koreanum* may play vital role on AChE inhibitory activity. In addition, other studies revealed that icariin has effect on improving dysfunction in spinal cord injury (Tohda and Nagata, 2012; Zhang et al., 2014) and neuroprotective effects (Chen et al., 2016; Yang et al., 2016). Moreover, Zong et al (2016) demonstrated that icariin attenuates ibotenic acid-induced excitotoxicity in rat hippocampus. Furthermore, icaritin was also reported to be a neuroprotective candidate (Wang et al., 2007; Jiang et al., 2016). Similarly, icariin and icaritin as well as other flavonol glycoside (epimedidin A, B and C) showed potent inhibitory activity on AChE in the present study.

To investigate inhibition mode of active compounds against AChE including icariin, icaritin, epimedidin A, epimedidin B and epimedidin C, the enzyme kinetics were performed. According to the results of kinetic analysis, all of the tested compounds showed noncompetitive type inhibition by decreasing the V_{max} values without changing the K_m values with K_i values ranging from 25.55 to 32.46 μ M (Table 8, Figure 14 and 15). The prediction of binding sites after the *in vitro* AChE assay using molecular docking studies showed that the binding sites between AChE and active compounds were similar compared with E2020, a known noncompetitive inhibitor (Figure 16). The gorge leading to the active site of AChE is performing as a “vacuum cleaner” confirming fast supply of the substrate molecules into the active site deeply buried in the AChE. Inhibitors may associate with a peripheral anionic site (PAS), remote from the active center, to influence

allosterically catalysis. The noncompetitive inhibition is caused by blocking the entrance of AChE in the gorge of active site resulting the binding of large inhibitors. When the inhibitor was combined with PAS, consisting of TYR70, ASP72, TYR121, TRP279 and TYR334, the conformational change of the AChE was occurred. At the same time, ACh receptor was not identified as a definite structure. The packing of inhibitor at the PAS prohibits the entrance of other molecules, even as small as water. The TRP84 residue is the anionic site which binds the quaternary ammonium of choline, and that of active center inhibitors (Bourne et al., 1995; Tougu, 2001; Massoulii et al., 1993; Dan et al., 2012). E2020, a known inhibitor for AChE, is a member of a large family of *N*-benzylpiperidine-based AChE inhibitors. E2020 offers the patient significant improvements by being administered only once a day and having fewer side effects. Furthermore, E2020 displays high selectivity for AChE in comparison to BChE. In addition, E2020 has a unique orientation along the active-site gorge, extending from the anionic subsite of the active site, at the bottom near TRP84, to the peripheral anionic site, at the top near TRP279 (Kryger et al., 1999). In the present study, E2020 forms only hydrophobic interaction with GLN69, TYR70, ASP72, SER81, TRP84, ASN85, TYR121, SER122, TRP279, ILE287, ARG289, PHE290, PHE330, PHE331, TYR334 and GLY335 (Table 9 and Figure 17A). Among the tested compounds, icariin exhibited the highest binding affinity with the -9.51 kcal/mol binding score. The oxygen and nitrogen groups of AChE residues were associated with hydrogen bonds with hydroxyl groups of icariin (Figure 17B), and the oxygen group of icaritin were involved in a hydrogen bonding with AChE (Figure 17C). Although the binding energies of epimedin A, epimedin B and epimedin C exhibited low values, the inhibitory activities of these compounds were comparable with icariin and icaritin (Table 6). The result of molecular docking simulation indicated that the tested compounds were interacted at the PAS. Thus, it was found that these compounds showed allosteric inhibition against AChE corresponding with the *in vitro* results of AChE inhibitory assay. From the structure

activity relationship (SAR), glycosylation at C-3 and C-7 of prenylated flavonol of *E. koreanum* might be essential to show anti-AChE activity.



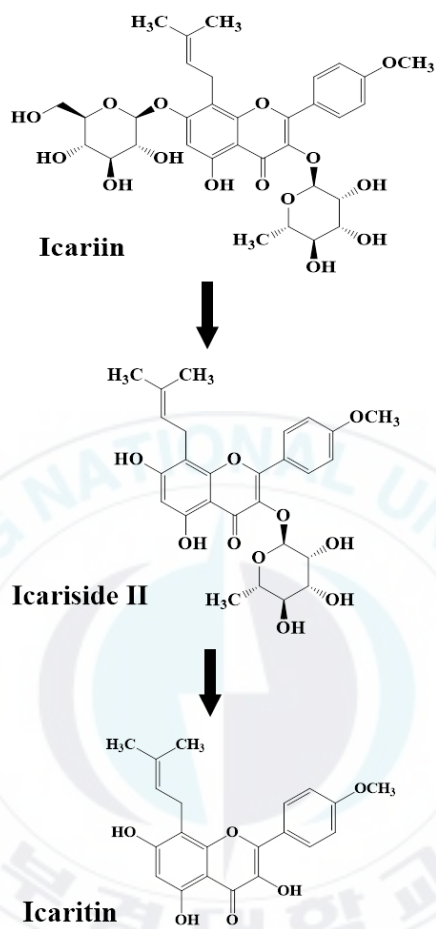


Figure 18. Proposed metabolic pathway of icariin in human intestine.

V. Conclusion

In conclusion, the results of current study confirmed that the aerial parts of *E. koreanum* and its constituents possess anti-DM and anti-AD properties. Comparative evaluation upon these activities of *E. koreanum* might be useful in the development of therapeutic agents for patients of DM and AD. Among the tested compounds, icaritin and icariside II, which are deglycosylated metabolites of icariin showed significant inhibitory activities on PTP1B and BACE1. In addition, icariin, epimedin A and epimedin C were appeared to be selective inhibitors of AChE. Furthermore, enzyme kinetic analysis and molecular docking simulation study supported the preceding results. Thus, the computational study and experimental validation can help to develop new natural drug candidates against diabetes and Alzheimer's disease, providing awesome basis for the application of active compounds as drug candidates for treatment of DM and AD. In addition, further investigations for the bioactivity of these natural products may prove therapeutic or preventive potential of *E. koreanum* and its constituents in the pathological situations *in vivo*.

VI. References

- Bao, H., and Chen, L. (2011). [Icariin reduces mitochondrial oxidative stress injury in diabetic rat hearts]. *Zhongguo Zhong yao za zhi= Zhongguo zhongyao zazhi= China journal of Chinese materia medica*, 36(11), 1503-1507.
- Barman, A., and Prabhakar, R. (2013). Elucidating the catalytic mechanism of β -secretase (BACE1): a quantum mechanics/molecular mechanics (QM/MM) approach. *Journal of Molecular Graphics and Modelling*, 40, 1-9.
- Bartus, R. T., Dean, R. L., Beer, B., and Lipka, A. S. (1982). The cholinergic hypothesis of geriatric memory dysfunction. *Science*, 217(4558), 408-414.
- Baskaran, S. K., Goswami, N., Selvaraj, S., Muthusamy, V. S., and Lakshmi, B. S. (2012). Molecular dynamics approach to probe the allosteric inhibition of PTP1B by chlorogenic and cichoric acid. *Journal of chemical information and modeling*, 52(8), 2004-2012.
- Berman, H. M., Battistuz, T., Bhat, T. N., Bluhm, W. F., Bourne, P. E., Burkhardt, K., Feng, Z., Gilliland, G. L., Iype, L., Jain, S., Fagan, P., Marvin, J., Padilla, D., Ravichandran, B., Thanki, N., Weissig, H., Westbrook, J. D., and Zardecki, C. (2002). The protein data bank. *Acta Crystallographica Section D: Biological Crystallography*, 58(6), 899-907.
- Bernstein, F. C., Koetzle, T. F., Williams, G. J., Meyer, E. F., Brice, M. D., Rodgers, J. R., Kennard, O., Shimanouchi, T., and Tasumi, M. (1977). The protein data bank: a computer-based archival file for macromolecular structures. *European Journal of Biochemistry*, 80(2), 319-324.
- Bond, M., Rogers, G., Peters, J., Anderson, R., Hoyle, M., Miners, A., Moxham, T., Davis, S., Thokala, P., Wailoo, A., and Jeffreys, M. (2012). The effectiveness and

- cost-effectiveness of donepezil, galantamine, rivastigmine and memantine for the treatment of Alzheimer's disease (review of Technology Appraisal No. 111): a systematic review and economic model.
- Bourne, Y., Taylor, P., and Marchot, P. (1995). Acetylcholinesterase inhibition by fasciculin: crystal structure of the complex. *Cell*, 83(3), 503-512.
- Butterfield, D. A., Reed, T., Newman, S. F., and Sultana, R. (2007). Roles of amyloid β -peptide-associated oxidative stress and brain protein modifications in the pathogenesis of Alzheimer's disease and mild cognitive impairment. *Free Radical Biology and Medicine*, 43(5), 658-677.
- Chen, X. J., Tang, Z. H., Li, X. W., Xie, C. X., Lu, J. J., and Wang, Y. T. (2015). Chemical constituents, quality control, and bioactivity of epimedii folium (Yinyanghuo). *The American Journal of Chinese Medicine*, 43(05), 783-834.
- Chen, Y., Deng, Y., Zhang, B., and Gong, C. X. (2014). Deregulation of brain insulin signaling in Alzheimer's disease. *Neuroscience bulletin*, 30(2), 282-294.
- Chen, Y. J., Zheng, H. Y., Huang, X. X., Han, S. X., Zhang, D. S., Ni, J. Z., and He, X. Y. (2016). Neuroprotective Effects of Icariin on Brain Metabolism, Mitochondrial Functions, and Cognition in Triple-Transgenic Alzheimer's Disease Mice. *CNS Neuroscience & Therapeutics*, 22(1), 63-73.
- Chiba, S. (1997). Molecular mechanism in α -glucosidase and glucoamylase. *Bioscience, biotechnology, and biochemistry*, 61(8), 1233-1239.
- Cho, N. J., Sung, S. H., Lee, H. S., Jeon, M. H., and Kim, Y. C. (1995). Anti-hepatotoxic activity of icariside II, a constituent of *Epimedium koreanum*. *Archives of Pharmacal Research*, 18(4), 289-292.
- Cho, W. K., Kim, H., Choi, Y. J., Yim, N. H., Yang, H. J., and Ma, J. Y. (2012). *Epimedium koreanum* Nakai water extract exhibits antiviral activity against porcine epidermic diarrhea virus in vitro and in vivo. *Evidence-Based Complementary and Alternative Medicine*, 2012.

- Choi, C. W., Choi, Y. H., Cha, M. R., Yoo, D. S., Kim, Y. S., Yon, G. H., Hong, K. S., Kim, Y. H., and Ryu, S. Y. (2010). Yeast α -glucosidase inhibition by isoflavones from plants of Leguminosae as an in vitro alternative to acarbose. *Journal of agricultural and food chemistry*, 58(18), 9988-9993.
- Choi, J. S., Ali, M. Y., Jung, H. A., Oh, S. H., Choi, R. J., and Kim, E. J. (2015). Protein tyrosine phosphatase 1B inhibitory activity of alkaloids from Rhizoma Coptidis and their molecular docking studies. *Journal of ethnopharmacology*, 171, 28-36.
- Cornish-Bowden, A. (1974). A simple graphical method for determining the inhibition constants of mixed, uncompetitive and non-competitive inhibitors. *Biochemical Journal*, 137(1), 143-144.
- Cui, L., Na, M., Oh, H., Bae, E. Y., Jeong, D. G., Ryu, S. E., Kim, S., Kim, B. Y., Oh, W. K., and Ahn, J. S. (2006). Protein tyrosine phosphatase 1B inhibitors from Morus root bark. *Bioorganic & medicinal chemistry letters*, 16(5), 1426-1429.
- Dan, C., Yu-ren, J., Chuan-jun, L., Ya-fei, P., and Yun-feng, X. (2012). *Virtual screening of acetylcholinesterase inhibitors*. INTECH Open Access Publisher.
- Darvesh, S., Hopkins, D. A., and Geula, C. (2003). Neurobiology of butyrylcholinesterase. *Nature Reviews Neuroscience*, 4(2), 131-138.
- Dickson, D. W., Crystal, H. A., Bevana, C., Honer, W., Vincent, I., and Davies, P. (1995). Correlations of synaptic and pathological markers with cognition of the elderly. *Neurobiology of aging*, 16(3), 285-298.
- Dixon, Á. (1953). The determination of enzyme inhibitor constants. *Biochemical journal*, 55(1), 170.
- Elchebly, M., Payette, P., Michaliszyn, E., Cromlish, W., Collins, S., Loy, A. L., Normandin, D., Cheng, A., Himms-Hagen, J., Chan, C. C., Ramachandran, C., Gresser, M. J., Tremblay, M. L., and Kennedy, B. P. (1999). Increased insulin sensitivity and obesity resistance in mice lacking the protein tyrosine phosphatase-1B gene. *Science*, 283(5407), 1544-1548.

- Ellman, G. L., Courtney, K. D., Andres, V., and Featherstone, R. M. (1961). A new and rapid colorimetric determination of acetylcholinesterase activity. *Biochemical pharmacology*, 7(2), 88-95.
- Etxeberria, U., de la Garza, A. L., Campión, J., Martínez, J. A., and Milagro, F. I. (2012). Antidiabetic effects of natural plant extracts via inhibition of carbohydrate hydrolysis enzymes with emphasis on pancreatic alpha amylase. *Expert opinion on therapeutic targets*, 16(3), 269-297.
- Feng, H. L., Dang, H. Z., Fan, H., Chen, X. P., Rao, Y. X., Ren, Y., Yang, J. D., Shi, J., Wang, Q. W., and Tian, J. Z. (2016). Curcumin ameliorates insulin signalling pathway in brain of Alzheimer's disease transgenic mice. *International journal of immunopathology and pharmacology*, 29(4), 734.
- Ferri, C. P., Prince, M., Brayne, C., Brodaty, H., Fratiglioni, L., Ganguli, M., Hall, K., Hasegawa, K., Hendrie, H., Huang, Y., Jorm, A., Mathers, C., Menezes, P. R., Rimmer, E., and Sczufca, M. (2006). Global prevalence of dementia: a Delphi consensus study. *The lancet*, 366(9503), 2112-2117.
- Gandy, S. (2011). Perspective: prevention is better than cure. *Nature*, 475(7355), S15-S15.
- Gavin III, J. R., Alberti, K. G. M. M., Davidson, M. B., and DeFronzo, R. A., Drash, A., Gabbe, S. G., Genuth, S., Harris, M. I., Kahn, R., Keen, H., Knowler, W. C., Lebovitz, H., Maclaren N. K., Parmer, J. P., Raskin, P., Rizza, R. A., and Stern, M. P. (1997). Report of the expert committee on the diagnosis and classification of diabetes mellitus. *Diabetes care*, 20(7), 1183.
- Greig, N. H., Utsuki, T., Yu, Q. S., Zhu, X., Holloway, H. W., Perry, T., Lee, B., Ingram, D. K., and Lahiri, D. K. (2001). A new therapeutic target in Alzheimer's disease treatment: attention to butyrylcholinesterase. *Current medical research and opinion*, 17(3), 159-165.

- Guo, Y., Zhang, X., Meng, J., and Wang, Z. Y. (2011). An anticancer agent icaritin induces sustained activation of the extracellular signal-regulated kinase (ERK) pathway and inhibits growth of breast cancer cells. *European journal of pharmacology*, 658(2), 114-122.
- Hernández-Rodríguez, M., Correa-Basurto, J., Gutiérrez, A., Vitorica, J., and Rosales-Hernández, M. C. (2016). Asp32 and Asp228 determine the selective inhibition of BACE1 as shown by docking and molecular dynamics simulations. *European Journal of Medicinal Chemistry*, 124, 1142-1154.
- Herrmann, N., Chau, S. A., Kircanski, I., and Lanctôt, K. L. (2011). Current and emerging drug treatment options for Alzheimer's disease. *Drugs*, 71(15), 2031-2065.
- Hong, L., Koelsch, G., Lin, X., Wu, S., Terzyan, S., Ghosh, A. K., Zhang, X. C., and Tang, J. (2000). Structure of the protease domain of memapsin 2 (β -secretase) complexed with inhibitor. *Science*, 290(5489), 150-153.
- Huang, D., Yang, J., Lu, X., Deng, Y., Xiong, Z., and Li, F. (2013). An integrated plasma and urinary metabonomic study using UHPLC–MS: Intervention effects of *Epimedium koreanum* on 'Kidney-Yang Deficiency syndrome' rats. *Journal of pharmaceutical and biomedical analysis*, 76, 200-206.
- Huang, X., Zhu, D., and Lou, Y. (2007). A novel anticancer agent, icaritin, induced cell growth inhibition, G 1 arrest and mitochondrial transmembrane potential drop in human prostate carcinoma PC-3 cells. *European journal of pharmacology*, 564(1), 26-36.
- Huang, Z., Mou, L., Shen, Q., Lu, S., Li, C., Liu, X., Wang, G., Li, S., Geng, L., Liu, Y., Wu, K., Chen, G., and Zhang, J. (2014). ASD v2. 0: updated content and novel features focusing on allosteric regulation. *Nucleic acids research*, 42(D1), D510-D516.
- International Diabetes Federation. IDF Diabetes Atlas, seventh edition 2015. [online], <http://www.idf.org/idf-diabetes-atlas-seventh-edition> (2015).

- Islam, M. N., Kim, U., Kim, D. H., Dong, M. S., and Yoo, H. H. (2012). High-performance liquid chromatography-based multivariate analysis to predict the estrogenic activity of an Epimedium koreanum extract. *Bioscience, biotechnology, and biochemistry*, 76(5), 923-927.
- Jiang, M. C., Chen, X. H., Zhao, X., Zhang, X. J., and Chen, W. F. (2016). Involvement of IGF-1 receptor signaling pathway in the neuroprotective effects of Icaritin against MPP⁺-induced toxicity in MES23.5 cells. *European journal of pharmacology*, 786, 53-59.
- Johnson, T. O., Ermolieff, J., and Jirousek, M. R. (2002). Protein tyrosine phosphatase 1B inhibitors for diabetes. *Nature Reviews Drug Discovery*, 1(9), 696-709.
- Jung, H. J., Jung, H. A., Min, B. S., and Choi, J. S. (2015). Anticholinesterase and β -Site Amyloid Precursor Protein Cleaving Enzyme 1 Inhibitory Compounds from the Heartwood of Juniperus chinensis. *Chemical and Pharmaceutical Bulletin*, 63(11), 955-960.
- Kang, H. K., Choi, Y. H., Kwon, H., Lee, S. B., Kim, D. H., Sung, C. K., Park, Y. I., and Dong, M. S. (2012). Estrogenic/antiestrogenic activities of a Epimedium koreanum extract and its major components: in vitro and in vivo studies. *Food and Chemical Toxicology*, 50(8), 2751-2759.
- Keum, J. H., Han, H. Y., Roh, H. S., Seok, J. H., Lee, J. K., Jeong, J., Kim, J. A., Woo, M. H., Choi, J. S., and Min, B. S. (2014). Analysis and stability test of the extracts from Epimedium Herba, Atractylodis Rhizoma Alba and Polygalae Radix for toxicity study. *Kor. J. Pharmacogn*, 45, 135-140.
- Kryger, G., Silman, I., and Sussman, J. L. (1999). Structure of acetylcholinesterase complexed with E2020 (Aricept®): implications for the design of new anti-Alzheimer drugs. *Structure*, 7(3), 297-307.

- Kumar, K. M., Anbarasu, A., and Ramaiah, S. (2014). Molecular docking and molecular dynamics studies on β -lactamases and penicillin binding proteins. *Molecular BioSystems*, 10(4), 891-900.
- Kwon, J. H., Chang, M. J., Seo, H. W., Lee, J. H., Min, B. S., Na, M., Kim, J. C., Woo, M. H., Choi, J. S., Lee, H. K., and Bae, K. (2008). Triterpenoids and a sterol from the stem-bark of *Styrax japonica* and their protein tyrosine phosphatase 1B inhibitory activities. *Phytotherapy research*, 22(10), 1303-1306.
- Lee, M. K., Choi, Y. J., Sung, S. H., Shin, D. I., Kim, J. W., and Kim, Y. C. (1995). Antihepatotoxic activity of icariin, a major constituent of *Epimedium koreanum*. *Planta medica*, 61(06), 523-526.
- Lee, S., and Wang, Q. (2007). Recent development of small molecular specific inhibitor of protein tyrosine phosphatase 1B. *Medicinal research reviews*, 27(4), 553-573.
- Li, B., Stribley, J. A., Ticu, A., Xie, W., Schopfer, L. M., Hammond, P., Brimijoin, S., Hinrichs, S. H., and Lockridge, O. (2000). Abundant tissue butyrylcholinesterase and its possible function in the acetylcholinesterase knockout mouse. *Journal of neurochemistry*, 75(3), 1320-1331.
- Li, S., Zhang, J., Lu, S., Huang, W., Geng, L., Shen, Q., and Zhang, J. (2014). The mechanism of allosteric inhibition of protein tyrosine phosphatase 1B. *PloS one*, 9(5), e97668.
- Li, T., Zhang, X. D., Song, Y. W. and Liu, J. W. (2005). A microplate-based screening method for alpha-glucosidase inhibitors. *Chin. J. Clin. Pharmacol. Ther.* 10, 1128-1134
- Li, W. K., Pan, J. Q., Lü, M. J., Zhang, R. Y., and Xiao, P. G. (1995). A 9, 10-dihydrophenanthrene derivate from *Epimedium koreanum*. *Phytochemistry*, 39(1), 231-233.

- Li, W. K., Xiao, P. G., and Pan, J. Q. (1998). Complete assignment of ¹H and ¹³C NMR spectra of Ikarisoside A and epimodoside C. *Magnetic resonance in chemistry*, 36(4), 303-304.
- Lin, X., LI, W. K., and XIAO, P. G. (1999). Effects of Icariside II from *Epimedium koreanum* on Tumour Cell Lines In-vitro. *Pharmacy and Pharmacology Communications*, 5(12), 701-703.
- Lineweaver, H., and Burk, D. (1934). The determination of enzyme dissociation constants. *Journal of the American Chemical Society*, 56(3), 658-666.
- Liu, Z. Q., Liu, T., Chen, C., Li, M. Y., Wang, Z. Y., Chen, R. S., Wei, G. X., Wang, X. Y., and Luo, D. Q. (2015). Fumosorinone, a novel PTP1B inhibitor, activates insulin signaling in insulin-resistance HepG2 cells and shows anti-diabetic effect in diabetic KKAY mice. *Toxicology and applied pharmacology*, 285(1), 61-70.
- M de la Monte, S. (2012). Brain insulin resistance and deficiency as therapeutic targets in Alzheimer's disease. *Current Alzheimer Research*, 9(1), 35-66.
- Ma, H., He, X., Yang, Y., Li, M., Hao, D., and Jia, Z. (2011). The genus *Epimedium*: an ethnopharmacological and phytochemical review. *Journal of ethnopharmacology*, 134(3), 519-541.
- Ma, P., Zhang, S., Su, X., Qiu, G., and Wu, Z. (2015). Protective effects of icariin on cisplatin-induced acute renal injury in mice. *American journal of translational research*, 7(10), 2105.
- Makarova, M. N., Pozharitskaya, O. N., Shikov, A. N., Tesakova, S. V., Makarov, V. G., and Tikhonov, V. P. (2007). Effect of lipid-based suspension of *Epimedium koreanum* Nakai extract on sexual behavior in rats. *Journal of Ethnopharmacology*, 114(3), 412-416.
- Massoulié, J., Pezzementi, L., Bon, S., Krejci, E., and Vallette, F. M. (1993). Molecular and cellular biology of cholinesterases. *Progress in neurobiology*, 41(1), 31-91.

- Meng, F., Xiong, Z., Jiang, Z., and Li, F. (2005). Osteoblastic proliferation stimulating activity of *Epimedium koreanum*. Nakai extracts and its flavonol glycosides. *Pharmaceutical biology*, 43(1), 92-95.
- Mesulam, M. M., Guillozet, A., Shaw, P., Levey, A., Duysen, E. G., and Lockridge, O. (2002). Acetylcholinesterase knockouts establish central cholinergic pathways and can use butyrylcholinesterase to hydrolyze acetylcholine. *neuroscience*, 110(4), 627-639.
- Murray, L. Protein Tyrosine Phosphatase 1B (PTP1B).
- Nakashima, K., Miyashita, H., Yoshimitsu, H., Fujiwara, Y., Nagai, R., and Ikeda, T. (2016). Two new prenylflavonoids from *Epimedium Herba* and their inhibitory effects on advanced glycation end-products. *Journal of natural medicines*, 70(2), 290-295.
- Nicholls, A., McGaughey, G. B., Sheridan, R. P., Good, A. C., Warren, G., Mathieu, M., Muchmore S. W., Brown, s. P., Grant, A., Haigh, J. A., and Nevins, N. (2010). Molecular shape and medicinal chemistry: a perspective. *Journal of medicinal chemistry*, 53(10), 3862-3886.
- Nordberg, A., Ballard, C., Bullock, R., Darreh-Shori, T., and Somogyi, M. (2013). A review of butyrylcholinesterase as a therapeutic target in the treatment of Alzheimer's disease. *Prim Care Companion CNS Disord*, 15(2).
- Oh, M. H., Houghton, P. J., Whang, W. K., and Cho, J. H. (2004). Screening of Korean herbal medicines used to improve cognitive function for anti-cholinesterase activity. *Phytomedicine*, 11(6), 544-548.
- Oh, T. W., Kang, S. Y., Kim, K. H., Song, M. Y., and Park, Y. K. (2013). Anti-diabetic effect of medicinal plants used for lower wasting-thirst in streptozotocin-induced diabetic rats. *The Korea Journal of Herbology*, 28(5), 53-60.
- Parthasarathy, R., Ilavarasan, R., and Karrunakaran, C. M. (2009). Antidiabetic activity of *Thespesia Populnea* bark and leaf extract against streptozotocin induced diabetic rats. *International Journal of PharmTech Research*, 1(4), 1069-1072.

- Pettersen, E. F., Goddard, T. D., Huang, C. C., Couch, G. S., Greenblatt, D. M., Meng, E. C., and Ferrin, T. E. (2004). UCSF Chimera—a visualization system for exploratory research and analysis. *Journal of computational chemistry*, 25(13), 1605-1612.
- Phan, M. A. T., Wang, J., Tang, J., Lee, Y. Z., and Ng, K. (2013). Evaluation of α -glucosidase inhibition potential of some flavonoids from *Epimedium brevicornum*. *LWT-Food Science and Technology*, 53(2), 492-498.
- Rao, A. A., Sridhar, G. R., and Das, U. N. (2007). Elevated butyrylcholinesterase and acetylcholinesterase may predict the development of type 2 diabetes mellitus and Alzheimer's disease. *Medical Hypotheses*, 69(6), 1272-1276.
- Schelterns, P., and Feldman, H. (2003). Treatment of Alzheimer's disease; current status and new perspectives. *The Lancet Neurology*, 2(9), 539-547.
- Selkoe, D. J. (2002). Alzheimer's disease is a synaptic failure. *Science*, 298(5594), 789-791.
- Seong, S. H., Roy, A., Jung, H. A., Jung, H. J., and Choi, J. S. (2016). Protein tyrosine phosphatase 1B and α -glucosidase inhibitory activities of *Pueraria lobata* root and its constituents. *Journal of Ethnopharmacology*, 194, 706-716.
- Shobana, S., Sreerama, Y. N., and Malleshi, N. G. (2009). Composition and enzyme inhibitory properties of finger millet (*Eleusine coracana* L.) seed coat phenolics: Mode of inhibition of α -glucosidase and pancreatic amylase. *Food Chemistry*, 115(4), 1268-1273.
- Tian, W., Lei, H., Guan, R., Xu, Y., Li, H., Wang, L., Yang, B., Gao, Z., and Xin, Z. (2015). Icariside II ameliorates diabetic nephropathy in streptozotocin-induced diabetic rats. *Drug design, development and therapy*, 9, 5147.
- Tohda, C., and Nagata, A. (2012). *Epimedium koreanum* extract and its constituent Icariin improve motor dysfunction in spinal cord injury. *Evidence-Based Complementary and Alternative Medicine*, 2012.

- Tougu, V. (2001). Acetylcholinesterase: mechanism of catalysis and inhibition. *Current Medicinal Chemistry-Central Nervous System Agents*, 1(2), 155-170.
- Van De Laar, F. A., Lucassen, P. L., Akkermans, R. P., Van De Lisdonk, E. H., Rutten, G. E., and Van Weel, C. (2005). α -Glucosidase Inhibitors for Patients With Type 2 Diabetes Results from a Cochrane systematic review and meta-analysis. *Diabetes care*, 28(1), 154-163.
- Wang, Z., Zhang, X., Wang, H., Qi, L., and Lou, Y. (2007). Neuroprotective effects of icaritin against beta amyloid-induced neurotoxicity in primary cultured rat neuronal cells via estrogen-dependent pathway. *Neuroscience*, 145(3), 911-922.
- Wiesmann, C., Barr, K. J., Kung, J., Zhu, J., Erlanson, D. A., Shen, W., Fahr, B. J., Zhong, M., Taylor, L., Randal, M and McDowell, R. S. (2004). Allosteric inhibition of protein tyrosine phosphatase 1B. *Nature structural & molecular biology*, 11(8), 730-737.
- Wu, H., Kim, M., and Han, J. (2016). Icariin Metabolism by Human Intestinal Microflora. *Molecules*, 21(9), 1158.
- Wu, H., Lien, E. J., and Lien, L. L. (2003). Chemical and pharmacological investigations of Epimedium species: a survey. In *Progress in Drug Research* (pp. 1-57). Birkhäuser Basel.
- Xin, H., Zhou, F., Liu, T., Li, G. Y., Liu, J., Gao, Z. Z., Bai, G. Y., Lu, H., and Xin, Z. C. (2012). Icariin ameliorates streptozotocin-induced diabetic retinopathy in vitro and in vivo. *International journal of molecular sciences*, 13(1), 866-878.
- Xu, H. B., and Huang, Z. Q. (2007). Vasorelaxant effects of icariin on isolated canine coronary artery. *Journal of cardiovascular pharmacology*, 49(4), 207-213.
- Yang, L. B., Lindholm, K., Yan, R., Citron, M., Xia, W., Yang, X. L., Beach, T., Sue, L., Wong, P., Price, D., and Li, R. (2003). Elevated β -secretase expression and enzymatic activity detected in sporadic Alzheimer disease. *Nature medicine*, 9(1), 3-4.

- Yang, P., Guan, Y. Q., Li, Y. L., Zhang, L., and Li, L. (2016). Icariin promotes cell proliferation and regulates gene expression in human neural stem cells in vitro. *Molecular medicine reports*.
- Yin, C., Deng, Y., Gao, J., Li, X., Liu, Y., and Gong, Q. (2016). Icariside II, a novel phosphodiesterase-5 inhibitor, attenuates streptozotocin-induced cognitive deficits in rats. *Neuroscience*, 328, 69-79.
- Youn, K., Lee, J., Ho, C. T., and Jun, M. (2016). Discovery of polymethoxyflavones from black ginger (*Kaempferia parviflora*) as potential β -secretase (BACE1) inhibitors. *Journal of Functional Foods*, 20, 567-574.
- Zhang, L., Shen, C., Chu, J., Zhang, R., Li, Y., and Li, L. (2014). Icariin decreases the expression of APP and BACE-1 and reduces the β -amyloid burden in an APP transgenic mouse model of Alzheimer's disease. *Int. J. Biol. Sci*, 10(2), 181-191.
- Zhang, W., Xing, B., Yang, L., Shi, J., and Zhou, X. (2015). Icaritin attenuates myocardial ischemia and reperfusion injury via anti-inflammatory and anti-oxidative stress effects in rats. *The American Journal of Chinese Medicine*, 43(06), 1083-1097.
- Zhang, X., Oh, M., Kim, S., Kim, J., Kim, H., Kim, S., Houghton, P. J., and Whang, W. (2013). Epimediphine, a novel alkaloid from *Epimedium koreanum* inhibits acetylcholinesterase. *Natural product research*, 27(12), 1067-1074.
- Zhou, J., Wu, J., Chen, X., Fortenbery, N., Eksioglu, E., Kodumudi, K. N., PK, E., Dong, J., Djeu, J. Y., and Wei, S. (2011). Icariin and its derivative, ICT, exert anti-inflammatory, anti-tumor effects, and modulate myeloid derived suppressive cells (MDSCs) functions. *International immunopharmacology*, 11(7), 890-898.
- Zong, N., Li, F., Deng, Y., Shi, J., Jin, F., and Gong, Q. (2016). Icariin, a major constituent from *Epimedium brevicornum*, attenuates ibotenic acid-induced excitotoxicity in rat hippocampus. *Behavioural Brain Research*, 313, 111-119.

감사의 글

이 논문이 완성되기까지 도움을 주신 많은 분들에게 짧은 글로써 감사한 마음을 전하고자 합니다.

먼저, 부족한 제가 더 나아갈 수 있도록 이끌어 주시고 따뜻한 관심과 아낌없는 가르침을 주신 최재수 지도교수님께 감사 드립니다. 교수님께서 보여주신 열정, 노력과 도전하는 자세를 잊지 않고 실천하여 더욱더 발전하는 사람이 되겠습니다.

또한 귀중한 시간을 내어 깊은 관심으로 논문 심사에 힘써주신 남택정 교수님, 정운주 교수님께 진심으로 감사 드리고, 석사 과정 동안 훌륭한 강의를 해주시고 따뜻한 조언을 해주신 류은순 교수님, 김형락 교수님, 김재일 교수님께도 감사 드립니다. 그리고 후배들을 언제나 격려 해주시고, 모범이 되어주신 전북대학교 정현아 교수님께도 감사한 마음을 전합니다.

학부 시절 동안 훌륭한 가르침을 주신 동의대학교 분자생물학과의 모든 교수님께 감사 드리며, 대학원 진학에 많은 도움을 주시고 응원해주신 한창희 교수님께 진심으로 감사 드립니다.

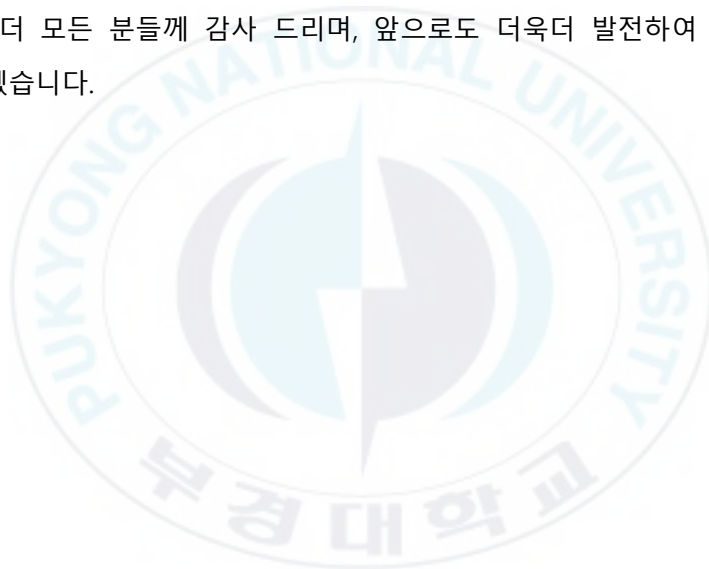
2년 남짓한 기간 동안 하루에 12시간 이상을 함께 보낸 실험실 선·후배님들께도 많은 것을 배우고 느꼈습니다. 거의 모든 것을 함께하며 힘이 되어준 희진이 언니, 수희 언니 항상 감사하고 있고, 가족들과 떨어져 타국에서 열심히 공부하며 많은 도움을 준 Ali, Abdul, Howlader, Susoma, Emon, Nisha, Himanshu, Anupom, 그리고 저보다 늦게 들어왔지만 잘 따라주고 많이 가르쳐 준 Pradeep, Ting, Prashamsa, Srijan, Zhou, Mondal에게도 감사한 마음을 전합니다. 또한 늦깎이 학생으로서 학업에 대단한 열정을 보여주신 조윤숙 약사님께도 감사 드리고, 산업 대학원생이지만 함께 실험하고 발

표도 같이 한 양파언니 수진 쌤도 감사 드립니다.

연락도 잘 안되고 자주 만나지도 못했지만 뒤에서 항상 응원해준 언니, 오빠, 친구, 동생들도 너무 감사합니다.

마지막으로 학부 졸업 후 대학원에 진학하겠다는 제 결정을 믿고 든든한 지원군, 버팀목이 되어준 사랑하는 가족, 아빠, 엄마, 언니, 오빠, 동생에게도 감사 드립니다. 항상 응원해주신 덕분에 이렇게 결실을 맺을 수 있었습니다.

다시 한번 더 모든 분들께 감사 드리며, 앞으로도 더욱더 발전하여 맛있는 사회인으로 성장하겠습니다.



2016년 12월

김 다 혜